

A kernelised Stein discrepancy for assessing the fit of inhomogeneous random graph models

Anum Fatima *

Department of Statistics
University of Oxford
Oxford, United Kingdom
fatima@stats.ox.ac.uk

Gesine Reinert

Department of Statistics
University of Oxford
Oxford, United Kingdom
reinert@stats.ox.ac.uk

Abstract

Complex data are often represented as a graph which in turn can often be viewed as a realisation of a random graph, such as of an inhomogeneous random graph model (IRG). For general fast goodness-of-fit tests in high dimensions, kernelised Stein discrepancy (KSD) tests are a powerful tool. Here, we develop, test, and analyse a KSD-type goodness-of-fit test for IRG models that can be carried out with a single observation of the network. The test is applicable to a network of any size, and does not depend on the asymptotic distribution of the test statistic. We also provide theoretical guarantees.

1 Introduction

Networks are often used to represent complex data for data mining in application areas such as transportation (Shekelyan et al. [2015], Åkerblom et al. [2023]), management (Chen et al. [2024], Bellamy and Basole [2013], Lee et al. [2018]), biology (Liu et al. [2017], Wang et al. [2014]), and social science (Kapucu and Demiroz [2011], Khademizadeh et al. [2025], Dinkelberg et al. [2025]). For example, social networks represent actors as vertices and the relations between them as edges. The edges in these networks are often random, with different probabilities for different edges. While many probabilistic models for random networks are available, see for example Newman [2018], learning such models from large data sets can be prohibitive. Instead, here we focus on models in which edges are assumed to occur independently of each other; this network model is known as the inhomogeneous random graph model (IRG). Under additional assumptions on how edge probabilities arise, model fitting in an IRG is often computationally feasible; see, for example, Santos et al. [2021], Liu et al. [2025] and Karwa et al. [2024]. Particular instances are stochastic blockmodels with known vertex classes, as well as degree-corrected stochastic blockmodels suggested in Karrer and Newman [2011]. However, for downstream tasks such as edge validation, it is important that the fitted model actually fits the data reasonably well. How can we assess such a fit?

Classical statistical goodness-of-fit tests based, for example, on chi-square asymptotics can show poor performance in high dimensions, see Arias-Castro et al. [2018]. A challenge is that, in contrast to standard settings with independent and identically distributed (i.i.d.) data, in network analysis, usually only one data point, that is, one network, is available. For this setting, Dan and Bhattacharya [2020] propose a test based on the spectral norm of the (scaled) observed adjacency matrix of the graph, which yields a test statistic that in their asymptotic regime approximately follows a standard Tracy-Widom distribution. However, the asymptotic distribution of the test statistic depends on the sparsity regime of the network, see for example Chakrabarty et al. [2021], and a prior. For a given network, it is not clear which regime to use. Moreover, likelihood ratio tests based on the assumption

*Lecturer of Statistics, Lahore College for Women University (LCWU), Lahore, Pakistan. Alternative email: anumfatimam@gmail.com

of independent edges, such as in Karwa et al. [2024], usually implicitly assume that the alternative model also has independent edges; in real networks, however, such as in friendship networks, edges may not occur independently of each other.

Based on the success of kernelised Stein discrepancy tests for high-dimensional continuous i.i.d. data, developed in Chwialkowski et al. [2016] and Liu et al. [2016], Xu and Reinert [2021] devised the so-called *graph kernel Stein statistic* (gKSS) to assess the fit of exponential random graph models given a single observed network, employing theoretical results from Reinert and Ross [2019]. This test does not require any assumptions on an asymptotic regime. In this paper, we use a similar strategy to develop a gKSS-type test for assessing goodness-of-fit for IRG models, with theoretical guarantees. Our method assumes that the features of all vertices, on which edge probabilities depend, are known in advance and are not estimated as part of the testing procedure. We illustrate the method on synthetic as well as real-world networks. Our experiments show that this gKSS-type test outperforms likelihood-based tests for contaminated synthetic networks, and it gives plausible results for four real networks, which are often used for benchmarking, namely Lazega’s lawyers network from Lazega [2001], the Karate club network from Zachary [1977], the Florentine marriage network from Padgett [1987], and the Dolphin network from Lusseau et al. [2003]. Our main contributions are as follows.

1. We provide a novel goodness-of-fit test for IRG models.
2. We illustrate on synthetic data that the test can outperform likelihood-based tests on networks with dependent edges.
3. We show that on four real networks, the test gives plausible results.
4. We provide theoretical guarantees for the test procedure.

The code for the experiments can be found at IRG-gKSS.

2 Background

2.1 Inhomogeneous random graph models

An IRG model, as proposed in Bollobás et al. [2007], is a model for a simple, unweighted, undirected graph $\mathcal{G} = (\mathcal{V}, \mathcal{E})$ with vertex set \mathcal{V} , of size n and edge set \mathcal{E} . The graph can be represented by a collection of 0-1 entries $\mathbf{x} = (x_{u,v}, 1 \leq u < v \leq n)$ of size $N = \binom{n}{2}$. We set $[N] = \{(u, v), 1 \leq u < v \leq n\}$ for the set of vertex pairs. Each vertex u has an associated value (or feature) g_u ; an edge between vertices u and v is assumed to occur with probability $p_{u,v} = \mathbb{P}((u, v) \in \mathcal{E} | g_u, g_v)$, independently of all other edges in the network. The edge probabilities can thus depend on features of the two vertices which the edge connects. With $s = (u, v) \in [N]$ denoting a vertex pair we write $p_s := p_{u,v} \in \Omega = [0, 1]^N$, and we denote $\mathbf{p} = \{p_{u,v}, u, v = 1, \dots, n\}$, the matrix of edge probabilities of all vertex pairs. The likelihood of \mathbf{x} under an IRG model with edge probability matrix \mathbf{p} , or short: under $\text{IRG}(\mathbf{p})$, is

$$\mathbb{P}(\mathbf{X} = \mathbf{x}) = \prod_{u < v=1}^n (1 - p_{u,v}) \left(\frac{p_{u,v}}{1 - p_{u,v}} \right)^{x_{u,v}}. \quad (1)$$

Two instances of IRG models that have attracted particular attention in network science run as follows. First, the Erdős-Rényi Mixture Models (ERMM), as introduced in Holland et al. [1983], is a special case of an IRG model with vertex set \mathcal{V} which is divided into L homogeneous groups of vertices, with the probability of an edge depending on the group membership of the vertices it connects. In this case, g_u is the group membership of the vertex u and is assumed known a priori for all the vertices in the network, and two vertices of types i and j form an edge with probability $Q_{i,j}$. Thus, the probability of an edge between a vertex u and v under ERMM is $p_{u,v} = Q_{g_u, g_v}$; we set $\mathbf{Q} = \{Q_{i,j}; i, j = 1, \dots, L\}$, which is an $L \times L$ symmetric matrix with entries in $[0, 1]$. In this paper we denote an ERMM with parameters \mathbf{n} and \mathbf{Q} by $\text{ERMM}(\mathbf{n}, \mathbf{Q})$, where $\mathbf{n} = \{n_i; i = 1, \dots, L\}$ is the vector of group sizes, so that $\sum_{i=1}^L n_i = n$.

The second special case of an IRG is the degree-corrected stochastic block model (DCSBM) by Karrer and Newman [2011]. It is an extension of ERMMs with inhomogeneous edge probabilities within each group. In the setting of ERMMs, a DCSBM, in addition, has as extra parameter a vector $\boldsymbol{\theta} = \{\theta_v\}_{v=1}^n$, and sets $p_{u,v} = \theta_u \theta_v Q_{g_u, g_v}$. To avoid complications arising when for estimated

parameters, $\theta_u \theta_v Q_{g_u, g_v} > 1$, we also consider the variant $p_{u,v} = 1 - e^{-\theta_u \theta_v Q_{g_u, g_v}}$. In sparse graphs, $1 - e^{-\theta_u \theta_v Q_{g_u, g_v}} \approx \theta_u \theta_v Q_{g_u, g_v}$ and hence the DCSBM is an approximating model. This variant can be seen as the probability that a Poisson variable $X_{u,v}$ with mean $\theta_u \theta_v Q_{g_u, g_v}$ is at least 1. Indeed for parameter estimation it is convenient to assume that the number of edges between distinct vertices u and v follows a Poisson distribution with mean $\theta_u \theta_v Q_{g_u, g_v}$, independently of the edge indicators for other vertex pairs, and that $X_{u,u}$ follows a Poisson distribution with mean $\theta_u^2 Q_{g_u, g_u}/2$. When fitting a DCSBM to data we use this Poissonized version, as implemented in Karrer and Newman [2011].

2.2 Stein's method

Stein's method, originating in Stein [1972], provides a means to compare probability distributions through characterising operators. In a nutshell, for p a target distribution, a *Stein operator* \mathcal{A}_p with Stein class $\mathcal{F}(\mathcal{A}_p)$ is such that if X has distribution p (short: $X \sim p$) then $\mathbb{E}\mathcal{A}_p f(X) = 0$ for all $f \in \mathcal{F}(\mathcal{A}_p)$. If $W \sim q$ is any random element which is close in distribution to X , then intuitively, it should hold that $\mathbb{E}\mathcal{A}_p f(W) \approx 0$. In Gorham and Mackey [2015], it is proposed to quantify this intuition by assessing a so-called *Stein discrepancy*

$$S(p, q; \mathcal{H}) = \sup_{f \in \mathcal{H}} |\mathcal{A}_p f(W)|. \quad (2)$$

Choosing as \mathcal{H} the class of all Lipschitz-1 functions gives the Wasserstein-1 distance $\|p - q\|_1$.

2.3 Kernel Stein Discrepancies

Evaluating the supremum in (2) over a large class of functions, such as that needed for Wasserstein distance, is usually computationally not possible, as observed in Gorham and Mackey [2015]. Instead, to test the fit of a continuous distribution, Chwialkowski et al. [2016] and Liu et al. [2016] propose to use a so-called kernel Stein discrepancy, obtained by taking set \mathcal{H} as a reproducing kernel Hilbert space (RKHS) associated with kernel k , inner product $\langle \cdot, \cdot \rangle$ and unit ball $B_1(\mathcal{H})$. Let $Y \sim q$. Formally, the *kernel Stein discrepancy (KSD)* between p and q is given by $\text{KSD}(p, q; k) = \sup_{f \in B_1(\mathcal{H})} |\mathbb{E}[\mathcal{A}_p f(Y)]|$.

Under some assumptions, $\text{KSD}(p, q; k)$ can be evaluated explicitly. For a continuous pdf p , under suitable conditions, the operator $\mathcal{A}_p f(w) = \langle f(w), \nabla \log p(w) \rangle + \nabla f(w)$ is a Stein operator. Set $h_p(x, y) = \langle \mathcal{A}_p k(x, \cdot), \mathcal{A}_p k(\cdot, y) \rangle$. Then if Y, Y' are independent $\sim q$, we have $\text{KSD}(p, q; k)^2 = \mathbb{E}h_p(Y, Y')$. Moreover, in this continuous setting, if the distribution q is not available in closed form, then KSD can be estimated from samples $(y_i, y'_j)_{i,j=1,\dots,n}$ i.i.d. $\sim q$, and manipulations using the structure of the RKHS show that a natural estimator for $\text{KSD}(p, q; k)^2$ is given through $\widehat{\text{KSD}(p, q; k)^2} = \frac{1}{n^2} \sum_{i=1}^n \sum_{j=1}^n h_p(y_i, y'_j)$.

For assessing goodness of fit to network distributions, two complications arise: First, the distribution is discrete on the set of networks, and hence, a different Stein operator is needed. Second, there is often only one observed network; hence, the KSD cannot be easily estimated. In Section 3, we give a goodness-of-fit test for IRG models developed by borrowing the ideas from KSD.

2.4 Other goodness-of-fit tests for inhomogeneous random graph models

For an observed network \mathbf{y} with $q(\mathbf{y}) = \mathbb{P}(\mathbf{Y} = \mathbf{y})$, the true likelihood of the observed network, a classical goodness-of-fit test for a specific IRG among a larger class of IRGs is a generalised likelihood ratio test (GLR test), based on the ratio of the likelihoods (1) for the null model and the alternative model, to test the null hypothesis $H_0 : \mathbf{Y} \sim \text{ERMM}(\mathbf{n}, \mathbf{Q}_0)$ against a general IRG alternative model,

$$\Lambda = \frac{\prod_{u \leq v} (1 - p_{0;u,v})^{1-x_{u,v}} (p_{0;u,v})^{x_{u,v}}}{\max_{\mathbf{p} \in \Omega} \left(\prod_{s \leq r} (1 - p_{s,r})^{1-x_{s,r}} (p_{s,r})^{x_{s,r}} \right)}. \quad (3)$$

Then under the null hypothesis, $-2 \ln \Lambda$ is asymptotically χ_k^2 distributed where k is the number of free parameters under Ω . The GLR test here is a one-sided test, and we reject the null hypothesis at level α if $-2 \ln \Lambda > \chi_k^2(\alpha)$. In many test situations, this test is optimal, see Zeitouni et al. [1992]. However, it strongly relies on the alternative distribution being an IRG.

3 A Stein Goodness-of-fit Test

Here, we develop a KSD-type test for IRG models; theoretical guarantees are given in Section 5. Before we give our Stein operator and KSD test statistic, we introduce some notation. For a simple, unweighted, undirected graph $\mathcal{G} = (\mathcal{V}, \mathcal{E})$ with vertex set \mathcal{V} , of size n , and edge set \mathcal{E} , and collection of edge indicators $\mathbf{x} = (x_{u,v}) \in [N]$, as in Xu and Reinert [2021] we denote

$\mathbf{x}^{(s,1)}$, the collection with 1 at the s - coordinate and the same as \mathbf{x} otherwise,
 $\mathbf{x}^{(s,0)}$, the collection with 0 at the s - coordinate and the same as \mathbf{x} otherwise,
 \mathbf{x}_{-s} , the collection $\{x_{r,t}, 1 \leq r < t \leq n, (r,t) \neq (u,v)\}$, without the s - coordinate.

3.1 An IRG Stein operator

For a function $f : \{0, 1\}^N \rightarrow \mathbb{R}$ we set $\Delta_s f(\mathbf{x}) = f(\mathbf{x}^{(s,1)}) - f(\mathbf{x}^{(s,0)})$, and we set

$$\mathcal{A}_{\text{IRG}} f(\mathbf{x}) = \frac{1}{N} \sum_{s \in [N]} \mathcal{A}_{\text{IRG}}^{(s)} f(\mathbf{x}), \quad (4)$$

with

$$\mathcal{A}_{\text{IRG}}^{(s)} f(\mathbf{x}) = p_s \left(f(\mathbf{x}^{(s,1)}) - f(\mathbf{x}) \right) + (1 - p_s) \left(f(\mathbf{x}^{(s,0)}) - f(\mathbf{x}) \right). \quad (5)$$

A detailed theoretical underpinning of this operator choice can be found in Section A of the Supplementary Material.

Proposition 3.1. *For a graph $\mathcal{G} = (\mathcal{V}, \mathcal{E})$ with adjacency matrix $\mathbf{X} \sim \text{IRG}(\mathbf{p})$, the operator (4) is a Stein operator with Stein class $\mathcal{F}(\mathcal{A}) = \{f : \{0, 1\}^N \rightarrow \mathbb{R}\}$, that is, for all $f : \{0, 1\}^N \rightarrow \mathbb{R}$,*

$$\mathbb{E} \mathcal{A}_{\text{IRG}} f(\mathbf{X}) = 0. \quad (6)$$

The proof of this proposition follows in a straightforward way from the definition of a Stein operator and is deferred to Section B in the supplementary material.

3.2 A graph kernel Stein statistic for IRG models

As for an IRG, $\sup_{f \in B_1(\mathcal{H})} |\mathbb{E}[\mathcal{A}_{\text{IRG}} f(Y)]|$ is usually not observed, in analogy to Xu and Reinert [2021] we introduce the empirical IRG-graph kernel Stein statistic IRG-gKSS

$$\text{IRG-gKSS}(\mathbf{p}; \mathbf{x}) = \sup_{\|f\|_{\mathcal{H}} \leq 1} \left| \frac{1}{N} \sum_{s \in [N]} \mathcal{A}_{\text{IRG}}^{(s)} f(\mathbf{x}) \right|.$$

Here $f(\cdot) = \{f \in \mathcal{H} : \|f\|_{\mathcal{H}} \leq 1\}$ are functions in a unit ball of an RKHS with kernel K and inner product $\langle \cdot, \cdot \rangle$, and $\mathcal{A}_{\text{IRG}}^{(s)}$ is given in (5). Since the functions f are in the unit ball of the underlying RKHS, the supremum can be calculated exactly, giving

$$\text{IRG-gKSS}^2(\mathbf{p}; \mathbf{x}) = \frac{1}{N^2} \sum_{s, s' \in [N]} h_{\mathbf{x}}(s, s'), \quad (7)$$

with $h_{\mathbf{x}}(s, s') = \left\langle \mathcal{A}_{\text{IRG}}^{(s)} K(\mathbf{x}, \cdot), \mathcal{A}_{\text{IRG}}^{(s')} K(\cdot, \mathbf{x}) \right\rangle$. For large networks, evaluating (7) can be computationally intensive. As in Xu and Reinert [2021], an edge re-sampling procedure can instead be used. When re-sampling a fixed number B of vertex pairs from the network, let $s_b, b = 1, \dots, B$, be the edge samples from $[N]$. We then set as re-sampled Stein operator

$$\widehat{\mathcal{A}_{\text{IRG}}^B} f(\mathbf{x}) = \frac{1}{B} \sum_{b \in [B]} \mathcal{A}_{\text{IRG}}^{(s_b)} f(\mathbf{x}) \quad (8)$$

and estimate it by

$$\widehat{\text{IRG-gKSS}}^2(\mathbf{p}; \mathbf{x}) = \frac{1}{B^2} \sum_{b, b' \in [B]} h_{\mathbf{x}}(s_b, s_{b'}'), \quad (9)$$

where $h_{\mathbf{x}}(s_b, s_{b'}') = \left\langle \mathcal{A}_{\text{IRG}}^{(s_b)} K(\mathbf{x}, \cdot), \mathcal{A}_{\text{IRG}}^{(s_{b'}')} K(\cdot, \mathbf{x}) \right\rangle$. We use test statistic (7) and (9) as a statistic for a Monte Carlo goodness-of-fit testing procedure. The detailed test procedure is given in the next subsection.

Algorithm 1 Goodness-of-fit to test the fit of $\text{IRG}(\mathbf{p}_0)$

Input: Observed network \mathbf{x} ,
null edge probably matrix, \mathbf{p}_0 ,
size of null set M ,
choice of graph kernel,
for $i = 1$ **to** M **do**
 Simulate M networks from $\text{IRG}(\mathbf{p}_0)$
 Compute a set ϕ of IRG-gKSS^2 using (7) from the simulated networks
end for
Find the empirical quantiles $\gamma_{\alpha/2}$ and $\gamma_{1-\alpha/2}$ from the set ϕ
Compute $\phi = \text{IRG-gKSS}^2(\mathbf{p}_0; \mathbf{x})$ using (7), from the observed network \mathbf{x}
Output: If $\phi < \gamma_{\alpha/2}$ or $\phi > \gamma_{1-\alpha/2}$ reject the hypothesis that the $\text{IRG}(\mathbf{p}_0)$ fits the observed network against a general alternative.

Algorithm 2 Goodness-of-fit to test the fit of $\text{IRG}(\mathbf{p}_0)$ with edge re-sampling

Input: Observed network \mathbf{x} ,
null edge probably matrix, \mathbf{p}_0 ,
re-sampling size B ,
size of null set M ,
choice of graph kernel,
for $i = 1$ **to** M **do**
 Simulate M networks from $\text{IRG}(\mathbf{p}_0)$
 Compute a set ϕ of $\widehat{\text{IRG-gKSS}}^2$ given in (9), from a sample of vertex pairs $s_{1,i}, \dots, s_{B,i}$,
 chosen uniformly at random and with replacement, from each simulated network.
end for
Find the empirical quantiles $\gamma_{\alpha/2}$ and $\gamma_{1-\alpha/2}$ from the set ϕ
Sample a set of vertex pairs $\{s_1, \dots, s_B\}$ uniformly at random and with replacement from the
observed network \mathbf{x}
Compute $\phi = \widehat{\text{IRG-gKSS}}^2(\mathbf{p}_0; \mathbf{x})$ using only the sample of vertex pairs as given in (9)
Output: If $\phi < \gamma_{\alpha/2}$ or $\phi > \gamma_{1-\alpha/2}$ reject the hypothesis that the $\text{IRG}(\mathbf{p}_0)$ fits the observed
network against a general alternative.

3.3 The Goodness-of-fit Testing Procedure

For an observed network \mathbf{x} , for which we want to assess the fit to an $\text{IRG}(\mathbf{p}_0)$, i.e. to test the hypothesis $H_0 : \mathbf{X} \sim \text{IRG}(\mathbf{p}_0)$, against a general alternative, we carry out a Monte Carlo test using Algorithm 1.

For large networks, we use IRG-gKSS with edge re-sampling as given in Algorithm 2. In all these tests, γ_α is used to denote the empirical α -quantile of the set of test statistics computed from the networks simulated under $\text{IRG}(\mathbf{p}_0)$. Ties are broken at random, and interpolation is used when required.

We note that this test is a pure significance test, in the sense that only the distribution under the null hypothesis is specified. In contrast, a generalised likelihood ratio test would also specify a parametric distribution under the alternative hypothesis. We do not detail here how the null hypothesis is obtained; sometimes it is determined from first principles, and sometimes a parametric model with learned parameter values is used, see for example Liu et al. [2025].

3.4 Choice of Kernel in IRG-gKSS

The calculated values of IRG-gKSS statistics depend on the kernel used and its corresponding RKHS. Following Xu and Reinert [2021], since the operator in (4) embeds a notion of conditional probability, we use a vector-valued reproducing kernel Hilbert space (vvRKHS) introduced in Xu and Reinert [2021] as graph kernels to separate the treatment of x_s and x_{-s} . For more details on vvRKHS

and graph kernels, see the supplementary material of Xu and Reinert [2021]. Section C in the supplementary material provides a detailed discussion on kernel choice.

4 Applications

In this section, we give applications of the IRG-gKSS test. First, we use simulated networks before we illustrate the results for real-world benchmark networks.

4.1 Synthetic data experiments: Planting anomalies

For the experiments in this section, we simulate synthetic networks from an $\text{IRG}(\mathbf{p})$ model, plant anomalies, and test the fit of $\text{IRG}(\mathbf{p})$ on these networks with anomalies to assess the test performance in detecting anomalies in the network. In all experiments, we simulate $m = 50$ networks for each setting and record the proportion of times the test rejects the fit of the null model. All tests are carried out at the 5% level of significance. In the Monte Carlo setup, we simulate $M = 200$ networks for each null model to obtain the null set ϕ for that model and use the same set to test its fit on all simulated networks. The shaded area around each point is a confidence band computed using $\hat{p} \pm 2\hat{p}(1 - \hat{p})/m$, where \hat{p} is the proportion of times the test rejects the null hypothesis in m repetitions of the test. In this section, to calculate IRG-gKSS we use the WL kernel with $h = 3$. A discussion about the effect of the graph kernel used to calculate IRG-gKSS is given in Section E of the supplementary material.

Implementation Details All experiments are executed on a PC with an Intel(R) Core(TM) i7-4790S CPU and 16.0 GB RAM. Using our R code, a single computation of IRG-gKSS^2 (WL kernel with $h = 3$) for a network, simulated from an $\text{ERMM}(\mathbf{n}, \mathbf{Q})$ with \mathbf{n} and \mathbf{Q} given in next section, takes 13.69 seconds. Further discussion about the computation time is given in Section D of the supplementary material.

4.1.1 Experiment 1: Planted hubs

In this experiment, we simulate networks from an $\text{ERMM}(\mathbf{n}, \mathbf{Q})$ model, with $\mathbf{n} = (25, 25)$ and $\mathbf{Q} = \begin{pmatrix} 0.20 & 0.01 \\ 0.01 & 0.20 \end{pmatrix}$, plant hubs (vertices with high degree) in the simulated networks without much disturbing the edge density, using Algorithms 3 and 4 given in Section E of the supplementary material, and test the fit of $\text{ERMM}(\mathbf{n}, \mathbf{Q})$ on these networks with planted hubs. In this experiment, k is the number by which we try to increase the degree of the selected vertex to turn it into a hub, and R is the number of repetitions of the Algorithm 4, intended to create R hubs in the network. Note that the original increase in the degree and number of hubs created might not be equal to k and R if the network cannot accommodate these choices because of not enough edges. For more details, see Section E in the supplementary material. The results of our experiment, illustrated in Figure 1, show that IRG-gKSS can detect some deviation from the model with independent edges even when R , the intended number of hubs, is as low as 3, and k , the intended increase in the degree of selected hub vertices, is as low as 4.

In contrast, the GLR test fails to detect such an anomaly. While the number of edges in the simulated network is fixed, planting hubs introduces heterogeneity. We report the maximum degree as an indicator for the heterogeneity. The larger the heterogeneity, the easier it is for IRG-gKSS to detect the difference; for the GLR test, increased heterogeneity has no advantage. More results for this experiment, with different parameter settings, are given in Section E of the supplementary material.

4.1.2 Experiment 2: Planted cliques

Next, we simulate $\text{ER}(50, 0.06)$ networks and attempt to plant a clique of size K (a complete subgraph of K vertices) in each of these networks; if there are not enough edges, then the network is not used. We then test the fit of the $\text{ER}(50, 0.06)$ model on these networks with a planted clique. The results of this experiment are illustrated in Figure 2. Again, IRG-gKSS detects deviation from the ER structure when K is at least 7, while the GLR test again fails to detect the discrepancy. The results for more parameter settings are given in Section E of the supplementary material.

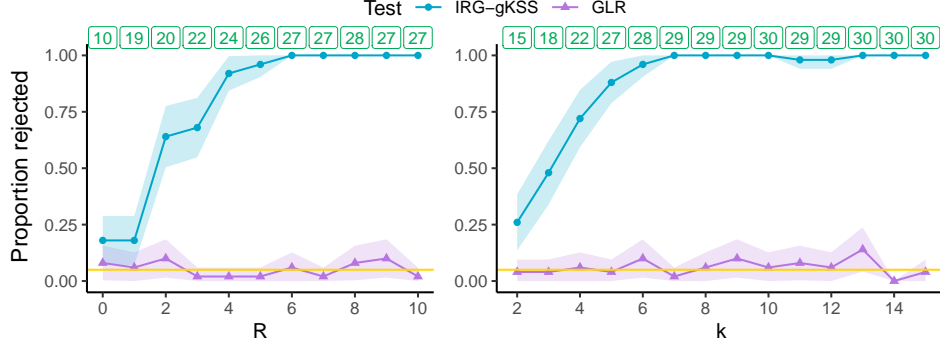


Figure 1: Power of the test to assess the fit of an $\text{ERMM}(\mathbf{n}, \mathbf{Q})$ to the network of size 50 with planted hubs. The numbers in boxes at the top of the plot are the average maximum degree observed in m repetitions of the test for each setting on the x-axis. Left: we fix $k = 4$ and let R vary; right: we fix $R = 3$ and let k vary.

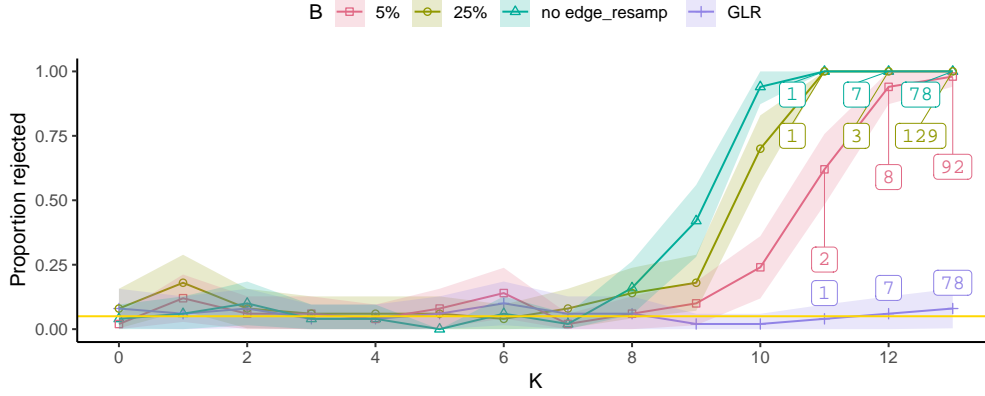


Figure 2: Power of the tests for the fit of an $\text{ER}(50, 0.06)$ to the network of size 50 with a planted clique using different proportions of edge resampling as well as no edge resampling version of the test statistic. The numbers in the boxes are the total number of networks sampled from the $\text{ER}(50, 0.06)$ model that had the number of edges less than $\binom{K}{2}$ to plant a clique of size K and were, therefore, not used in the experiment. The number is the total of $m = 50$ repetitions of the goodness-of-fit test.

4.2 Real Data Applications

In this section, we use IRG-gKSS to test the fit of IRG models to two network data sets, Lazega’s lawyers network from Lazega [2001] and Zachary’s karate club network from Zachary [1977]. The results for the Florentine marriage network and the Dolphin network are given in Section F of the supplementary material.

4.2.1 Lazega’s lawyers network

Lazega’s lawyers’ network is a dataset from a network study of a corporate law partnership that was carried out in a Northeastern US corporate law firm in New England. This data set is used to create a working network, an advice network, and a friendship network between the 71 attorneys (vertices) of this firm. Various vertex attributes are also part of the dataset, including seniority, formal status, gender, office in which they work, years with the firm, age, practice, and law school they attended. For more details, see Lazega [2001].

In this example, we test the fit of different IRG models to the three networks in the data set and record the results in Table 1.

Table 1: Goodness of fit results for testing the fit of IRG models on Lazega’s lawyers’ networks

| Networks | Group labels | ERMM | | DCSBM | |
|------------|--------------|------------------------|---------|------------------------|---------|
| | | IRG-gKSS ² | P-value | IRG-gKSS ² | P-value |
| Work | Single group | 4.356 (4.192,5.253) | 0.22886 | - | - |
| Advice | Single group | 15.15 (14.43,16.05) | 0.77612 | - | - |
| Friendship | Single group | 4.605 (4.923,6.028) | 0.02985 | 3.277 (2.816,3.620) | 0.71642 |
| | Status | 3.934 (4.135,5.143) | 0.02985 | 2.710 (2.253,2.928) | 0.42786 |
| | Office | 3.947 (3.833,4.852) | 0.13930 | - | - |

Table 2: Testing the fit of some IRG models on Zachary’s Karate club network

| | Model | | | |
|-----------------------|--------------------------|--------------------------------------|--------------------------------------|---|
| | ER(n, p) | ERMM($\mathbf{n}_1, \mathbf{Q}_1$) | ERMM($\mathbf{n}_2, \mathbf{Q}_2$) | DCSBM($\mathbf{n}, \mathbf{Q}, \theta$) |
| IRG-gKSS ² | 2.649 (0.9042,2.1097) | 1.937 (0.6215,1.507) | 1.553 (0.4553,1.106) | 1.053 (0.2793,0.7102) |
| P-value | 0.00995 | 0.00995 | 0.00995 | 0.00995 |

IRG-gKSS does not reject the fit of corresponding ER models for the Work and Advice networks, but rejects the fit of an ER model for the Friendship network. For the Friendship network, the test does not reject the fit of an ERMM with groups created according to the office where the lawyers work. For groups constructed using the status of the lawyers, the test rejects the fit of the corresponding ERMM, but does not reject the fit of a DCSBM. The test results for the ERMMs and DCSBMs with groups constructed using other vertex attributes are given in Section F of the supplementary material. The parameters for all the null models used in this example are in Section F of the supplementary material.

4.2.2 The Karate club network

Zachary’s karate club network from Zachary [1977] is a friendship network of 34 members of a karate club at a US university, which split into two factions as a result of an internal dispute (the group memberships after the split are shown in 23). This network is often used as a benchmark network dataset for community detection algorithms. Karrer and Newman [2011] fit a stochastic block model (SBM) and a degree-corrected stochastic block model (DCSBM) to this network. For this data set, the test proposed by Karwa et al. [2024] rejects the fit of ERMM with two groups and does not reject ERMM with four groups.

In this example, we test the fit of an ER, an ERMM, and a DCSBM to the karate club network. The parameters used for the null models are given in Section F of the supplementary material. The results of the IRG-gKSS test, given in Table 2, reject all four models, ER, ERMM with two groups, ERMM with four groups and the DCSBM, for the karate club network.

5 Theoretical properties of IRG-gKSS

An advantage of the KSD approach is that it is possible to provide theoretical guarantees. We take a unit ball of an RKHS \mathcal{H} with kernel K and inner product $\langle \cdot, \cdot \rangle$; for kernels satisfying Assumptions 5.1, Theorem 5.2 addresses the asymptotic distribution of the test statistic $\text{IRG-gKSS}^2(\mathbf{p}, \mathbf{x})$ in (7).

Assumption 5.1. For the kernel $K : \{0, 1\}^N \times \{0, 1\}^N \rightarrow \mathbb{R}$ of an RKHS \mathcal{H} , and a family of kernels $l_s : \{0, 1\} \times \{0, 1\} \rightarrow \mathbb{R}$, for $s \in [N]$, with an associated RKHS denoted by \mathcal{H}_s ,

1. \mathcal{H} is a tensor product RKHS, $\mathcal{H} = \otimes_{s \in [N]} \mathcal{H}_s$;
2. k is a product kernel, $k(x, y) = \otimes_{s \in [N]} l_s(x_s, y_s)$;
3. $\langle l_s(x_s, \cdot), l_s(x_s, \cdot) \rangle_{\mathcal{H}_s} = 1$;

4. $l_s(1, \cdot) - l_s(0, \cdot) \neq 0$ for all $s \in [N]$.

Theorem 5.2. *Let $\mathbf{x} \sim \text{IRG}(\mathbf{p})$, set $\mu = \mathbb{E}(\text{IRG-gKSS}^2(\mathbf{p}, \mathbf{x}))$, and $\sigma^2 = \text{Var}(\text{IRG-gKSS}^2(\mathbf{p}, \mathbf{x}))$. For $W = \frac{1}{\sigma}(\text{IRG-gKSS}^2(\mathbf{p}, \mathbf{x}) - \mu)$, and a standard normal random variable Z , under Assumption 5.1, the Wasserstein distance between the distributions satisfies*

$$\|\mathcal{L}(W) - \mathcal{L}(Z)\|_1 \leq \frac{C_1}{\sqrt{N}}, \quad (10)$$

where $C_1 = C_1(\mathbf{p}, K)$ is an explicit constant which depends on \mathbf{p} and the kernel K , but not on N .

Hence, for reasonably large networks, the test statistic (7) behaves like a normal random variable around its mean μ . Here is a sketch of the proof.

Proof. Under Assumptions 5.1, with $\alpha = (s, s'); s, s' \in [N]$, $\mathcal{I} = \{(s, s') : s, s' \in [N]\}$ and $|\mathcal{I}| = N^2$, we write (7) as an average of locally dependent random variables

$$X_\alpha = \frac{1}{N^2}(p_s - Y_s)(p_{s'} - Y_{s'})\langle l_s(Y_s, \cdot), l_{s'}(Y_{s'}, \cdot) \rangle c(s, s').$$

Here $\mathbf{Y} = (Y_s, s \in [N]) \in \{0, 1\}^N$ denotes a random vector representing edge indicators in an $\text{IRG}(\mathbf{p})$ graph of size n , and $c(s, s') = \langle l_s(1, \cdot) - l_s(0, \cdot), l_{s'}(1, \cdot) - l_{s'}(0, \cdot) \rangle$, which does not depend on Y_s or $Y_{s'}$. With $\mu_\alpha = \mathbb{E}X_\alpha$, we define the standardised count $W = \sum_{\alpha \in \mathcal{I}} (X_\alpha - \mu_\alpha) / \sigma$, which has zero mean and unit variance. Using the bound from Theorem 4.13, p.134, of Chen et al. [2011] and simplifying gives (10). The detailed proof is in Section B of the supplementary material. \square

For large networks, the use of IRG-gKSS in (7) is not economical and often not possible. Instead, we can estimate the test statistic from a sample of edges from the observed network using the edge re-sampling version of the statistic given in (9). We can re-write the test statistic in (9) by defining a count k_s , the number of times the vertex pair s is included in the sample \mathcal{B} , with $|\mathcal{B}| = B$, as

$$\widehat{\text{IRG-gKSS}}^2(\mathbf{p}; \mathbf{x}) = \frac{1}{B^2} \sum_{s, s' \in [N]} k_s k_{s'} h_{\mathbf{x}}(s_b, s'_b). \quad (11)$$

In this version of statistic, the randomness lies only in the counts $\mathbf{K} = (k_s, s \in [N])$, which are exchangeable and follow a multinomial distribution. Hence, the statistic (11) is a sum of weakly dependent random variables. Proposition 2 in Xu and Reinert [2021] proves that, for any fixed network \mathbf{x} and a fixed sampling fraction $F = B/N$, as $N \rightarrow \infty$ the statistic $\widehat{\text{IRG-gKSS}}^2(\mathbf{p}; \mathbf{x})$ is approximately normal with approximate mean $\text{IRG-gKSS}^2(\mathbf{p}; \mathbf{x})$.

6 Conclusion

In this paper, we develop IRG-gKSS , a KSD-type goodness-of-fit test for IRG models that does not require more than one observation of the network and that does not depend on any assumption on the asymptotic regime. We also give theoretical guarantees on IRG-gKSS for any size of the network.

IRG-gKSS is developed for simple, undirected random graphs in which the edges occur with a Bernoulli distribution with probabilities given by the edge probability matrix defined in the null hypothesis. Hence, we only test a simple null hypothesis with pre-specified edge probabilities. Testing a general null hypothesis would require a variation of this test that accommodates this generality and is one of the future directions of this research.

Moreover, the performance of IRG-gKSS depends on the type of graph kernel used with it. If the underlying graph kernel does not capture the structure of the network, the test does not detect any structural anomalies. Hence, the graph kernel to be used needs to be chosen carefully. Future research will address this issue and will include IMQ -type kernels as in Kanagawa et al. [2023]. Furthermore, IRG-gKSS is computationally expensive for even moderately large networks, and we need to use an edge-resampling version of the test statistic, while to some extent, sacrificing the power of the test. Speeding up the code by exploiting more parallelisation and fast matrix product algorithms will also be addressed in future work.

This paper presents work whose goal is to advance the field of Machine Learning. While there are many potential societal consequences of our work, through its contribution to a better understanding of machine learning algorithms, we feel that none of these warrants to be specifically highlighted here.

Acknowledgements and Disclosure of Funding The authors would like to thank Wenkai Xu for helpful discussions. AF is supported by the Commonwealth Scholarship Commission, United Kingdom, and in part by the UKRI EPSRC grant EP/X002195/1. This research was funded in whole, or in part, by the UKRI EPSRC grants EP/T018445/1, EP/R018472/1, EP/X002195/1 and EP/Y028872/1. For the purpose of Open Access, the authors note that a CC BY public copyright licence applies to any Author Accepted Manuscript version arising from this submission.

References

- N. Åkerblom, F. S. Hoseini, and M. Haghiri Chehreghani. Online learning of network bottlenecks via minimax paths. *Machine Learning*, 112:131–150, 2023.
- E. Arias-Castro, B. Pelletier, and V. Saligrama. Remember the curse of dimensionality: the case of goodness-of-fit testing in arbitrary dimension. *Journal of Nonparametric Statistics*, 30:448–471, 2018.
- A. D. Barbour. Stein’s method and Poisson process convergence. *Journal of Applied Probability*, 25 (A):175–184, 1988.
- M. A. Bellamy and R. C. Basole. Network analysis of supply chain systems: A systematic review and future research. *Systems Engineering*, 16:235–249, 2013.
- V. D. Blondel, J.-L. Guillaume, R. Lambiotte, and E. Lefebvre. Fast unfolding of communities in large networks. *Journal of Statistical Mechanics: Theory and Experiment*, 2008:P10008, 2008.
- B. Bollobás, S. Janson, and O. Riordan. The phase transition in inhomogeneous random graphs. *Random Structures & Algorithms*, 31:3–122, 2007.
- R. L. Breiger and P. E. Pattison. Cumulated social roles: The duality of persons and their algebras. *Social Networks*, 8:215–256, 1986.
- A. Caimo and N. Friel. Bayesian inference for exponential random graph models. *Social Networks*, 33:41–55, 2011.
- A. Chakrabarty, R. S. Hazra, F. den Hollander, and M. Sfragara. Spectra of adjacency and Laplacian matrices of inhomogeneous Erdős–Rényi random graphs. *Random Matrices: Theory and Applications*, 10:2150009, 2021.
- L. H. Y. Chen, L. Goldstein, and Q.-M. Shao. *Normal Approximation by Stein’s Method*, volume 2. Springer: Verlag, Berlin, Heidelberg, 2011.
- Y. Chen, C. U. Lehmann, and B. Malin. Digital information ecosystems in modern care coordination and patient care pathways and the challenges and opportunities for AI solutions. *Journal of Medical Internet Research*, 26:e60258, 2024.
- K. Chwialkowski, H. Strathmann, and A. Gretton. A kernel test of goodness of fit. In M. F. Balcan and K. Q. Weinberger, editors, *Proceedings of The 33rd International Conference on Machine Learning*, volume 48 of *Proceedings of Machine Learning Research*, pages 2606–2615, New York, New York, USA, 20–22 Jun 2016. PMLR.
- S. Dan and B. B. Bhattacharya. Goodness-of-fit tests for inhomogeneous random graphs. In H. D. III and A. Singh, editors, *Proceedings of the 37th International Conference on Machine Learning*, volume 119 of *Proceedings of Machine Learning Research*, pages 2335–2344. PMLR, 13–18 Jul 2020.
- A. Dinkelberg, B. S. Santana, and A. L. C. Bazzan. Endorsement networks in the 2022 Brazilian presidential elections: a case study on Twitter data. *Journal of the Brazilian Computer Society*, 31: 219–228, 2025.

- J. Gorham and L. Mackey. Measuring sample quality with Stein's method. In C. Cortes, N. Lawrence, D. Lee, M. Sugiyama, and R. Garnett, editors, *Advances in Neural Information Processing Systems*, volume 28. Curran Associates, Inc., 2015.
- F. Götze. On the rate of convergence in the multivariate CLT. *The Annals of Probability*, 19:724–739, 1991.
- P. W. Holland, K. B. Laskey, and S. Leinhardt. Stochastic blockmodels: First steps. *Social Networks*, 5:109–137, 1983.
- I. H. Jin, Y. Yuan, and F. Liang. Bayesian analysis for exponential random graph models using the adaptive exchange sampler. *Statistics and Its Interface*, 6:559–576, 2013.
- H. Kanagawa, W. Jitkrittum, L. Mackey, K. Fukumizu, and A. Gretton. A kernel Stein test for comparing latent variable models. *Journal of the Royal Statistical Society Series B: Statistical Methodology*, 85:986–1011, 2023.
- N. Kapucu and F. Demiroz. Measuring performance for collaborative public management using network analysis methods and tools. *Public Performance & Management Review*, 34:549–579, 2011.
- B. Karrer and M. E. J. Newman. Stochastic blockmodels and community structure in networks. *Physical Review E*, 83:016107, 2011.
- V. Karwa, D. Pati, S. Petrović, L. Solus, N. Alexeev, M. Raič, D. Wilburne, R. Williams, and B. Yan. Monte carlo goodness-of-fit tests for degree corrected and related stochastic blockmodels. *Journal of the Royal Statistical Society Series B: Statistical Methodology*, 86:90–121, 2024.
- S. Khademizadeh, A. Sajid, A. Q. Khan, F. Shoukat, and W. Hussain. Sentiment analysis of users tweets for polarity opinions detection using deep learning for health care service. In *AIoT Innovations in Digital Health*, pages 1–24. CRC Press; Boca Raton, 1st edition, 2025.
- N. M. Kriege, F. D. Johansson, and C. Morris. A survey on graph kernels. *Applied Network Science*, 5:6, 2020.
- E. Lazega. *The Collegial Phenomenon: The Social Mechanisms of Cooperation Among Peers in a Corporate Law Partnership*. Oxford University Press: New York, 2001.
- C.-Y. Lee, H.-Y. Chong, P.-C. Liao, and X. Wang. Critical review of social network analysis applications in complex project management. *Journal of Management in Engineering*, 34:04017061, 2018.
- J. Liu, M. Li, Y. Pan, W. Lan, R. Zheng, F.-X. Wu, and J. Wang. Complex brain network analysis and its applications to brain disorders: A survey. *Complexity*, 2017:8362741, 2017.
- Q. Liu, J. Lee, and M. Jordan. A kernelized Stein discrepancy for goodness-of-fit tests. In M. F. Balcan and K. Q. Weinberger, editors, *Proceedings of The 33rd International Conference on Machine Learning*, volume 48 of *Proceedings of Machine Learning Research*, pages 276–284, New York, New York, USA, 20–22 Jun 2016. PMLR.
- X. Liu, W. Song, K. Musial, Y. Li, X. Zhao, and B. Yang. Stochastic block models for complex network analysis: A survey. *ACM Transactions on Knowledge Discovery from Data*, 19:55, 2025.
- D. Lusseau. The emergent properties of a dolphin social network. *Proceedings of the Royal Society of London. Series B: Biological Sciences*, 270:S186–S188, 2003.
- D. Lusseau, K. Schneider, O. J. Boisseau, P. Haase, E. Slooten, and S. M. Dawson. The bottlenose dolphin community of Doubtful Sound features a large proportion of long-lasting associations: Can geographic isolation explain this unique trait? *Behavioral Ecology and Sociobiology*, 54: 396–405, 2003.
- M. Newman. *Networks*. Oxford University Press: New York, 2nd edition, 2018.
- G. Ouyang, D. K. Dey, and P. Zhang. A mixed-membership model for social network clustering. *Journal of Data Science*, 21:508–522, 2023.

- J. F. Padgett. Social mobility in hieratic control systems. In R. Breiger, editor, *Social Mobility and Social Structure*. Cambridge University Press: New York, 1987.
- G. Reinert and N. Ross. Approximating stationary distributions of fast mixing Glauber dynamics, with applications to exponential random graphs. *The Annals of Applied Probability*, 29:3201–3229, 2019.
- S. d. S. Santos, A. Fujita, and C. Matias. Spectral density of random graphs: convergence properties and application in model fitting. *Journal of Complex Networks*, 9:cnab041, 2021.
- M. Shekelyan, G. Jossé, and M. Schubert. Linear path skylines in multicriteria networks. In *2015 IEEE 31st International Conference on Data Engineering*, pages 459–470, 2015.
- C. Stein. A bound for the error in the normal approximation to the distribution of a sum of dependent random variables. In L. M. L. Cam, J. Neyman, and E. L. Scott, editors, *Proceedings of the Sixth Berkeley Symposium on Mathematical Statistics and Probability, Volume 2: Probability Theory*, volume 6, pages 583–603. University of California Press, 1972.
- J. Wang, X. Peng, W. Peng, and F.-X. Wu. Dynamic protein interaction network construction and applications. *Proteomics*, 14:338–352, 2014.
- W. Xu and G. Reinert. A Stein goodness-of-test for exponential random graph models. In A. Banerjee and K. Fukumizu, editors, *Proceedings of The 24th International Conference on Artificial Intelligence and Statistics*, volume 130 of *Proceedings of Machine Learning Research*, pages 415–423. PMLR, 13–15 Apr 2021.
- W. W. Zachary. An information flow model for conflict and fission in small groups. *Journal of Anthropological Research*, 33:452–473, 1977.
- O. Zeitouni, J. Ziv, and N. Merhav. When is the generalized likelihood ratio test optimal? *IEEE Transactions on Information Theory*, 38:1597–1602, 1992.

A Stein's method for IRG models

Here we underpin the proposed IRG Stein operator given in (4). In order to support its use in a KSD-type test, we detail Stein's method for IRG models.

To construct a Stein operator we use the insight from Barbour [1988] and Götze [1991], that if \mathcal{L}_0 is the stationary distribution of a homogeneous Markov process, then under some regularity assumptions the generator of the Markov process is a Stein operator for \mathcal{L}_0 . The Markov chain we shall use here is a Glauber Markov chain, as follows.

For an IRG(\mathbf{p}) as in Subsection 2.1, with adjacency matrix \mathbf{X} , and $p_s = \mathbb{P}(s = (u, v) \in \mathcal{E} | g_u, g_v)$, the conditional probability of an edge at the s -coordinate (vertex pair) i.e. to have $x_s = 1$, given the rest of the graph, \mathbf{x}_{-s} , is

$$q(\mathbf{x}^{(s,1)} | \mathbf{x}_{-s}) = \frac{\mathbb{P}(\mathbf{X} = \mathbf{x}^{(s,1)})}{\mathbb{P}(\mathbf{X} = \mathbf{x}_{-s})} = p_s. \quad (12)$$

We define a Markov process $\{X(t)\}_{t \geq 0}$ with state space $\{0, 1\}^N$ as follows. Given the current state \mathbf{x} , each vertex pair in $[N]$ has a clock which rings at i.i.d. exponentially distributed times with mean N , independently of the network. When the clock rings for a vertex pair $s \in [N]$ we resample the edge indicator x_s , setting an edge at s with probability $q(\mathbf{x}^{(s,1)} | \mathbf{x}_{-s}) = p_s$ and not setting an edge at s with probability $1 - p_s$. We then resample the edge indicator for the next vertex pair for which their clock rings and continue this process, which gives a Markov process $(\mathbf{X}(t), t \geq 0)$ in continuous time. The generator of the Markov process is

$$\mathcal{A}_{\text{IRG}} f(\mathbf{x}) = \frac{1}{N} \sum_{s \in [N]} \left[p_s \left(f(\mathbf{x}^{(s,1)}) - f(\mathbf{x}) \right) + (1 - p_s) \left(f(\mathbf{x}^{(s,0)}) - f(\mathbf{x}) \right) \right].$$

Proposition 3.1 shows that \mathcal{A}_{IRG} is an IRG Stein operator with Stein class $\mathcal{F}(\mathcal{A}) = \{f : \{0, 1\}^N \rightarrow \mathbb{R}\}$. We next illustrate its use for comparing different IRG models. To this purpose, we start with a so-called *Stein equation*. For this IRG Stein operator the Stein equation for a test function $h : \{0, 1\}^N \rightarrow \mathbb{R}$ is

$$\frac{1}{N} \sum_{s \in [N]} \left[p_s \Delta_s f(\mathbf{x}) + \left(f(\mathbf{x}^{(s,0)}) - f(\mathbf{x}) \right) \right] = h(\mathbf{x}) - \mathbb{E}h(\mathbf{X}). \quad (13)$$

For a given h , it is often possible to find a solution $f = f_h$ of (13). Then, for any random $\mathbf{W} \in \{0, 1\}^N$, replacing \mathbf{x} by \mathbf{W} and taking expectations gives

$$\mathbb{E}h(\mathbf{W}) - \mathbb{E}h(\mathbf{X}) = \frac{1}{N} \sum_{s \in [N]} \left[p_s \mathbb{E} \Delta_s f(\mathbf{W}) + \mathbb{E} \left(f(\mathbf{W}^{(s,0)}) - f(\mathbf{W}) \right) \right].$$

If the distribution of \mathbf{W} also has a Stein operator of the form (4), with parameters q_s , then

$$\mathbb{E}h(\mathbf{W}) - \mathbb{E}h(\mathbf{X}) = \frac{1}{N} \sum_{s \in [N]} (q_s - p_s) \mathbb{E} \Delta_s f(\mathbf{W}). \quad (14)$$

Thus, bounds on Δf_h , for $f = f_h$ solving (13) could be used to bound the difference in expectations $\mathbb{E}h(\mathbf{W}) - \mathbb{E}h(\mathbf{X})$. From Reinert and Ross [2019] the Stein equation (13) is solved by

$$f_h(\mathbf{x}) := - \int_0^\infty \mathbb{E} [h(\mathbf{X}(t)) - \mathbb{E}h(\mathbf{X}) | \mathbf{X}(0) = \mathbf{x}] dt \quad (15)$$

where $(\mathbf{X}(t), t \geq 0)$ is the above Glauber Markov chain. While Reinert and Ross [2019] provides a general framework of which IRG models can be seen as special cases, some of their results considerably simplify when, instead of a general exponential random graph model, an IRG model is used. As an instance, the next lemma gives the desired bounds on f_h in (15).

Lemma A.1. *For $f_h(\mathbf{x})$ in (15), the solution of the Stein equation (13) in (15), with \mathbf{X} following an IRG model, we have*

$$|\Delta_s f_h(\mathbf{x})| \leq \|\Delta_s h\| N. \quad (16)$$

Proof. Let $h : \{0, 1\}^N \rightarrow \mathbb{R}$ and f_h be given in (15). Suppose that $(U^{[\mathbf{x}, s]}(m), V^{[\mathbf{x}, s]}(m))$ is a coupling such that for $m \geq 0$, $\mathcal{L}(U^{[\mathbf{x}, s]}(m)) = \mathcal{L}(\mathbf{X}(m) | \mathbf{X}(0) = \mathbf{x}^{(s, 1)})$ and $\mathcal{L}(V^{[\mathbf{x}, s]}(m)) = \mathcal{L}(\mathbf{X}(m) | \mathbf{X}(0) = \mathbf{x}^{(s, 0)})$. Lemma 2.5 from Reinert and Ross [2019] gives

$$|\Delta_s f_h(\mathbf{x})| \leq \sum_{r \in [N], m \geq 0} \|\Delta_r h\| \mathbb{P}(U_r^{[\mathbf{x}, s]}(m) \neq V_r^{[\mathbf{x}, s]}(m)).$$

Since in an IRG, the edge indicators are independent, for $r \neq s$, we can take $U_r^{[\mathbf{x}, s]}(m) = V_r^{[\mathbf{x}, s]}(m)$, and thus

$$|\Delta_s f_h(\mathbf{x})| \leq \|\Delta_s h\| \sum_{m \geq 0} \mathbb{P}(U_s^{[\mathbf{x}, s]}(m) \neq V_s^{[\mathbf{x}, s]}(m)). \quad (17)$$

Now, let T be the first time a clock rings in the Glauber Markov process. Then $U^{[\mathbf{x}, s]}(T) = V^{[\mathbf{x}, s]}(T)$ and the two processes can be coupled to coincide after this time T , i.e. $U^{[\mathbf{x}, s]}(m) = V^{[\mathbf{x}, s]}(m)$ for $m \geq T$, while $U^{[\mathbf{x}, s]}(m) \neq V^{[\mathbf{x}, s]}(m)$ for $m < T$. Thus, $\mathbb{P}(U^{[\mathbf{x}, s]}(m) \neq V^{[\mathbf{x}, s]}(m)) = \mathbb{P}(T > m)$. By definition, $T \sim \text{Geometric}(\frac{1}{N})$ with $t = 1, 2, 3, \dots$, and so

$$\mathbb{P}(U_s^{[\mathbf{x}, s]}(m) \neq V_s^{[\mathbf{x}, s]}(m)) = \mathbb{P}(T > m) = \sum_{t=m+1}^{\infty} \left(1 - \frac{1}{N}\right)^{t-1} \frac{1}{N} = \left(1 - \frac{1}{N}\right)^m.$$

Using this result in (17) proves (16). \square

Employing the Stein equation and the solution of the Stein equation for a test function $h \in \mathcal{H}$ we can bound the Stein discrepancy (2) an $\text{IRG}(\mathbf{p})$ and an $\text{IRG}(\mathbf{p}^*)$ on the same set of vertices using (14); Theorem A.2 shows that the Stein discrepancy measures the similarity between the edge probabilities and thus provides a useful measure of similarity between two IRG models.

Theorem A.2. Let $\mathbf{X} \sim \text{IRG}(\mathbf{p})$ and $\mathbf{Y} \sim \text{IRG}(\mathbf{p}^*)$, where $p_s^* = \mathbb{P}(s = (u, v) \in \mathcal{E}^* | \ell_u, \ell_v)$, with ℓ_s encoding the features of the vertices in \mathbf{Y} . Then, for any test function $h : \{0, 1\}^N \rightarrow \mathbb{R}$,

$$|\mathbb{E}h(\mathbf{X}) - \mathbb{E}h(\mathbf{Y})| \leq \|\Delta h\| \sum_{s \in [N]} |p_s - p_s^*|. \quad (18)$$

In particular if $\mathcal{H} = \{h : \{0, 1\}^N \rightarrow \mathbb{R} : \|\Delta h\| \leq K(N)\}$ then

$$S(\text{IRG}(\mathbf{p}), \text{IRG}(\mathbf{p}^*), \mathcal{H}) \leq K(N) \sum_{s \in [N]} |p_s - p_s^*|.$$

Proof. For $\mathbf{Y} \sim \text{IRG}(\mathbf{p}^*)$ the Stein equation, as in (13), is

$$\frac{1}{N} \sum_{s \in [N]} \left[p_s^* \Delta_s f(\mathbf{y}) + \left(f(\mathbf{y}^{(s, 0)}) - f(\mathbf{y}) \right) \right] = h(\mathbf{y}) - \mathbb{E}h(\mathbf{Y}). \quad (19)$$

Next we use Lemma 2.4 in Reinert and Ross [2019] which gives that

$$|\mathbb{E}h(\mathbf{X}) - \mathbb{E}h(\mathbf{Y})| \leq \frac{1}{N} \sum_{s \in [N]} \mathbb{E} \left[|q_X(\mathbf{Y}^{(s, 1)} | \mathbf{Y}) - q_Y(\mathbf{Y}^{(s, 1)} | \mathbf{Y})| |\Delta_s f_h(\mathbf{Y})| \right], \quad (20)$$

where f_h is the solution of the Stein equation (13) for the distribution of \mathbf{X} . Hence, substituting the two transition probabilities in (20) and simplifying using (16) gives the bound (18). The bound for the Stein discrepancy is immediate. \square

As a special case, we compare two ERMM graphs, on the same set of vertices and also with the same group assignments, but possibly different edge probabilities. Its proof is immediate.

Corollary A.3. For $\mathbf{X} \sim \text{ERMM}(\mathbf{n}, \mathbf{Q})$ and $\mathbf{Y} \sim \text{ERMM}(\mathbf{n}^*, \mathbf{Q}^*)$, and for $g_s = \ell_s$ for all $s \in [N]$ the bound (18) simplifies to

$$|\mathbb{E}h(\mathbf{X}) - \mathbb{E}h(\mathbf{Y})| \leq \|\Delta h\| \sum_{i \leq j}^L N_{i,j} |Q_{i,j} - Q_{i,j}^*|,$$

Table 3: The bounds from (22) on the Stein discrepancies between IRG models for Lazega’s lawyers’ friendship network

| Group labels | Stein discrepancy with $K(N) = 3 * N^{-1}$ | | |
|--------------|--|--------|---------|
| | ER(n, p) to | | ERMM to |
| | ERMM | DCSBM | DCSBM |
| Single group | 0 | 0.5638 | - |
| Status | 0.5326 | 0.6517 | 0.5276 |
| Gender | 0.1940 | 0.5726 | 0.5576 |
| Office | 0.6155 | 0.6616 | 0.4713 |
| Practice | 0.2003 | 0.5698 | 0.5554 |
| Law school | 0.1717 | 0.5686 | 0.5571 |

where $N_{i,j} = \binom{n_i}{2}$ for $i = j$, $N_{i,j} = n_i n_j$ for $i \neq j$, $N = \sum_{i \leq j}^L N_{i,j}$, and L is the number of blocks. In particular, for $\mathbf{Z} \sim ER(n, p)$ and $\mathbf{X} \sim ERMM(\mathbf{n}, \mathbf{Q})$ and any $h : \{0, 1\}^N \rightarrow \mathbb{R}$, we bound

$$|\mathbb{E}h(\mathbf{X}) - \mathbb{E}h(\mathbf{Z})| \leq \|\Delta h\| \sum_{i \leq j}^L N_{i,j} |Q_{i,j} - p|. \quad (21)$$

Remark A.4. Functions h of interest are proportions of subgraphs of different types, where a count of a connected subgraph on $v \geq 2$ vertices is divided by n^v , as used in graphon convergence. For such functions h , the bound $\|\Delta h\| \leq O(N^{-1})$ shows that (21) is small when, on average, the edge probabilities in IRG are close to p .

As an example, we consider the test function h , in the bound (18), to be the proportion of triangles in the network; then $\|\Delta h\| \leq \frac{n-2}{\binom{n}{3}} = \frac{3}{\binom{n}{2}}$. Hence, the bound (18) simplifies to

$$|\mathbb{E}h(\mathbf{X}) - \mathbb{E}h(\mathbf{Y})| \leq \frac{3}{N} \sum_{s \in [N]} |p_s - p_s^*|. \quad (22)$$

Table 3 uses this bound to give distances between the models tested for fit for Lazega’s lawyers’ friendship network in Section 4 and Section F of this Supplementary Material, using $K(N) = 3N^{-1}$. For the Lazega’s lawyers’ friendship network with communities created using the law school which the lawyers attended, the discrepancy is smallest between an ER graph and an ERMM.

B Proofs of results stated in the main text

Proof of Proposition 3.1

For convenience, we restate the proposition here. For a graph $\mathcal{G} = (\mathcal{V}, \mathcal{E})$ with adjacency matrix $\mathbf{X} \sim \text{IRG}(\mathbf{p})$, the operator (4) is a Stein operator with Stein class $\mathcal{F}(\mathcal{A}) = \{f : \{0, 1\}^N \rightarrow \mathbb{R}\}$, that is, for all $f : \{0, 1\}^N \rightarrow \mathbb{R}$,

$$\mathbb{E}\mathcal{A}_{\text{IRG}}f(\mathbf{X}) = 0.$$

Proof. Using (5) we write

$$\begin{aligned} \mathbb{E}\mathcal{A}_{\text{IRG}}^{(s)}f(\mathbf{X}) &= \sum_{\mathbf{x}} \left[\mathbb{P}(\mathbf{X} = \mathbf{x}^{(s,0)}) \mathcal{A}_{\text{IRG}}^{(s)}f(\mathbf{x}^{(s,0)}) + \mathbb{P}(\mathbf{X} = \mathbf{x}^{(s,1)}) \mathcal{A}_{\text{IRG}}^{(s)}f(\mathbf{x}^{(s,1)}) \right] \\ &= \sum_{\mathbf{x}} \mathbb{P}(\mathbf{X}_{-s} = \mathbf{x}_{-s}) \left[(1 - p_s) \left\{ p_s \left(f(\mathbf{x}^{(s,1)}) - f(\mathbf{x}^{(s,0)}) \right) + (1 - p_s) \left(f(\mathbf{x}^{(s,0)}) - f(\mathbf{x}^{(s,0)}) \right) \right\} \right. \\ &\quad \left. + p_s \left\{ p_s \left(f(\mathbf{x}^{(s,1)}) - f(\mathbf{x}^{(s,1)}) \right) + (1 - p_s) \left(f(\mathbf{x}^{(s,0)}) - f(\mathbf{x}^{(s,1)}) \right) \right\} \right] \\ &= 0. \end{aligned}$$

Thus, $\mathbb{E}\mathcal{A}_{\text{IRG}}^{(s)}f(\mathbf{X}) = 0$, and with (4) we obtain the assertion. \square

Proof of Theorem 5.2

Before giving the proof we restate the result in Theorem 5.2: Let $\mathbf{x} \sim \text{IRG}(\mathbf{p})$, and set $\mu = \mathbb{E}(\text{IRG-gKSS}^2(\mathbf{p}, \mathbf{x}))$ and $\sigma^2 = \mathbb{V}\text{ar}(\text{IRG-gKSS}^2(\mathbf{p}, \mathbf{x}))$. For $W = \frac{1}{\sigma}(\text{IRG-gKSS}^2(\mathbf{p}, \mathbf{x}) - \mu)$, and a standard normal random variable Z , under Assumption 5.1 we have

$$\|\mathcal{L}(W) - \mathcal{L}(Z)\|_1 \leq \frac{C_1}{\sqrt{N}}, \quad (23)$$

where $C_1 = C_1(\mathbf{p})$ is an explicit constant which depends \mathbf{p} and the corresponding kernels.

Proof. For $s \in [N]$ in an $\text{IRG}(\mathbf{p})$, from (4)

$$\mathcal{A}_{\text{IRG}} f(\mathbf{x}) = \frac{1}{N} \sum_{s \in [N]} \left[p_s \Delta_s f(\mathbf{x}) + \left(f(\mathbf{x}^{(s,0)}) - f(\mathbf{x}) \right) \right] = \frac{1}{N} \sum_{s \in [N]} \mathcal{A}^{(s)} f(\mathbf{x}),$$

with

$$\mathcal{A}_{\text{IRG}}^{(s)} f(x) = p_s \left(f(x^{(s,1)}) - f(x) \right) + (1 - p_s) \left(f(x^{(s,0)}) - f(x) \right).$$

Thus, with (7),

$$\begin{aligned} \text{IRG-gKSS}^2(\mathbf{p}, x) &= \frac{1}{N^2} \sum_{s, s' \in [N]} \left\langle \mathcal{A}_{\text{IRG}}^{(s)} K(x, \cdot), \mathcal{A}_{\text{IRG}}^{(s')} K(x, \cdot) \right\rangle \\ &= \frac{1}{N^2} \sum_{s, s' \in [N]} \left\langle p_s \left(K(x^{(s,1)}, \cdot) - K(x, \cdot) \right) + (1 - p_s) \left(K(x^{(s,0)}, \cdot) - K(x, \cdot) \right), \right. \\ &\quad \left. p_{s'} \left(K(x^{(s',1)}, \cdot) - K(x, \cdot) \right) + (1 - p_{s'}) \left(K(x^{(s',0)}, \cdot) - K(x, \cdot) \right) \right\rangle. \end{aligned}$$

Under Assumption 5.1, we have

$$\begin{aligned} K(x^{(s,1)}, \cdot) - K(x, \cdot) &= (l_s(1, \cdot) - l_s(x_s, \cdot)) \prod_{t \neq s} l_t(x_t, \cdot) \\ &= (1 - x_s)(l_s(1, \cdot) - l_s(0, \cdot)) l_{s'}(x_{s'}, \cdot) \prod_{t \neq s, s'} l_t(x_t, \cdot), \end{aligned}$$

and

$$K(x^{(s,0)}, \cdot) - K(x, \cdot) = -x_s(l_s(1, \cdot) - l_s(0, \cdot)) l_{s'}(x_{s'}, \cdot) \prod_{t \neq s, s'} l_t(x_t, \cdot).$$

With these simplifications and $g(x^{-s, s'}, \cdot) := \prod_{t \neq s, s'} l_t(x_t, \cdot)$ gives

$$\begin{aligned} \text{IRG-gKSS}^2(\mathbf{p}, \mathbf{x}) &= \frac{1}{N^2} \sum_{s, s' \in [N]} (p_s(1 - x_s) - (1 - p_s)x_s)(p_{s'}(1 - x_{s'}) - (1 - p_{s'})x_{s'}) \\ &\quad \langle (l_s(1, \cdot) - l_s(0, \cdot)) l_{s'}(x_{s'}, \cdot), (l_{s'}(1, \cdot) - l_{s'}(0, \cdot)) l_s(x_s, \cdot) \rangle \langle g(x^{-s, s'}, \cdot), g(x^{-s, s'}, \cdot) \rangle \\ &= \frac{1}{N^2} \sum_{s, s' \in [N]} (p_s - x_s)(p_{s'} - x_{s'}) \langle (l_s(1, \cdot) - l_s(0, \cdot)) l_{s'}(x_{s'}, \cdot), (l_{s'}(1, \cdot) - l_{s'}(0, \cdot)) l_s(x_s, \cdot) \rangle \\ &= \frac{1}{N^2} \sum_{s, s' \in [N]} (p_s - x_s)(p_{s'} - x_{s'}) \langle l_s(x_s, \cdot), l_{s'}(x_{s'}, \cdot) \rangle c(s, s'). \end{aligned} \quad (24)$$

Here $c(s, s') = \langle l_s(1, \cdot) - l_s(0, \cdot), l_{s'}(1, \cdot) - l_{s'}(0, \cdot) \rangle$, which does not depend on x_s or $x_{s'}$, and Assumption 5.1 gives $\langle g(x^{-s, s'}, \cdot), g(x^{-s, s'}, \cdot) \rangle = 1$. With a random vector $\mathbf{Y} \in \{0, 1\}^N$, representing edge indicators in an $\text{IRG}(\mathbf{p})$ graph of size n , we write

$$X_\alpha = \frac{1}{N^2} (p_s - Y_s)(p_{s'} - Y_{s'}) \langle l_s(Y_s, \cdot), l_{s'}(Y_{s'}, \cdot) \rangle c(s, s').$$

Hence with $\alpha = (s, s')$; $s, s' \in [N]$, and $\mathcal{I} = \{(s, s') : s, s' \in [N]\}$ so that $|\mathcal{I}| = N^2$, using (24), we have

$$\text{IRG-gKSS}^2(\mathbf{p}, \mathbf{x}) = \sum_{\alpha \in \mathcal{I}} X_\alpha \text{ and } W = \sum_{\alpha \in \mathcal{I}} \frac{X_\alpha - \mu_\alpha}{\sigma}.$$

This representation writes IRG-gKSS^2 as an average of locally dependent random variables; to clarify the dependence, for any $\alpha, \beta \in \mathcal{I}$, X_α and X_β are independent unless α and β share at least one vertex pair. We note that W has zero mean and unit variance. Next, denoting the L_1 distance by $\|\cdot\|_1$, we apply Theorem 4.13, p.134, from Chen et al. [2011] to get a bound on between $\mathcal{L}(W)$ and $\mathcal{L}(Z)$, the distribution of a standard normal random variable Z , respectively, obtaining

$$\begin{aligned} \|\mathcal{L}(W) - \mathcal{L}(Z)\|_1 &\leq \sqrt{\frac{2}{\pi}} \mathbb{E} \left| \sum_{\alpha \in \mathcal{I}} (\xi_\alpha \eta_\alpha - \mathbb{E}(\xi_\alpha \eta_\alpha)) \right| + \sum_{\alpha \in \mathcal{I}} \mathbb{E} |\xi_\alpha \eta_\alpha|^2 \\ &\leq \sqrt{\frac{2}{\pi}} \sqrt{\text{Var}(\sum_{\alpha \in \mathcal{I}} \xi_\alpha \eta_\alpha)} + \sum_{\alpha \in \mathcal{I}} \mathbb{E} |\xi_\alpha \eta_\alpha|^2, \end{aligned} \quad (25)$$

with $\xi_\alpha = (X_\alpha - \mu_\alpha)/\sigma$, and $\eta_\alpha = \sum_{\beta \in A_\alpha} \xi_\beta$ where $A_\alpha = \{\beta = (t, t') \in \mathcal{I} : \alpha \cap \beta \neq \emptyset\} \subset \mathcal{I}$; we note that $|A_\alpha| = 2N - 1$.

To bound ξ_α and η_α , we first note that $|p_s - Y_s| \leq 1$, $\langle l_s(Y_s, \cdot), l_{s'}(Y_{s'}, \cdot) \rangle \leq 1$ and $c(s, s') \leq 4$ gives $|X_\alpha| \leq \frac{4}{N^2}$ and $|\mu_\alpha| \leq \frac{4}{N^2}$. So $\xi_\alpha \leq \frac{8}{N^2\sigma}$, $\eta_\alpha \leq \frac{16}{N\sigma}$, and

$$\sum_{\alpha \in \mathcal{I}} \mathbb{E} |\xi_\alpha \eta_\alpha|^2 \leq N^2 \times \frac{8}{N^2\sigma} \times \frac{256}{N^2\sigma^2} = \frac{2048}{N^2\sigma^3}.$$

Now $\sigma^2 = \sum_{\alpha \in \mathcal{I}} \text{Var} X_\alpha + \sum_{\alpha \in \mathcal{I}} \sum_{\beta \in A_\alpha} \text{Cov}(X_\alpha, X_\beta)$ with

$$\text{Var} X_\alpha = \frac{c(s, s')^2}{N^4} \text{Var}((p_s - Y_s)(p_{s'} - Y_{s'}) \langle l_s(Y_s, \cdot), l_{s'}(Y_{s'}, \cdot) \rangle) = \frac{c(s, s')^2}{N^4} f(p_s, p_{s'}),$$

where $f(p_s, p_{s'})$ is a function of the edge probabilities p_s and $p_{s'}$. Similarly the covariance term, for $\alpha = (s, s') \in \mathcal{I}$ and $\beta = (s, t) \in A_\alpha$ is

$$\begin{aligned} \text{Cov}(X_\alpha, X_\beta) &= \frac{c(\alpha)c(\beta)}{N^4} \mathbb{E}(p_s - Y_s)^2 (p_{s'} - Y_{s'}) (p_{gt} - Y_{gt}) \langle l_s(Y_s, \cdot), l_{s'}(Y_{s'}, \cdot) \rangle \langle l_s(Y_s, \cdot), l_t(Y_t, \cdot) \rangle \\ &\quad - \mu_\alpha \mu_\beta. \end{aligned}$$

Expanding the expectation and simplifying gives a covariance term of the form $c(\alpha, \beta, \mathbf{p})N^{-4}$. The first summation in σ^2 is over N^2 terms, and the number of summands for the covariance term is $N^2(2N - 1)$. Hence, the variance σ^2 is of order N^{-1} , and $\sum_{\alpha \in \mathcal{I}} \mathbb{E} |\xi_\alpha \eta_\alpha|^2$ is of order $N^{-\frac{1}{2}}$.

Now,

$$\text{Var} \left(\sum_{\alpha \in \mathcal{I}} \xi_\alpha \eta_\alpha \right) = \text{Var} \left(\sum_{\alpha \in \mathcal{I}} \sum_{\beta \in A_\alpha} \xi_\alpha \xi_\beta \right) = \sum_{\alpha \in \mathcal{I}} \sum_{\beta \in A_\alpha} \sum_{\gamma \in \mathcal{I}} \sum_{\delta \in A_\gamma} \text{Cov}(\xi_\alpha \xi_\beta, \xi_\gamma \xi_\delta),$$

is expanded in terms of the covariance of $\xi_\alpha \xi_\beta$ and $\xi_\gamma \xi_\delta$. This covariance is zero unless two of the 3-tuples of vertex pairs $\{\alpha, \beta\}$ and $\{\gamma, \delta\}$ share at least one vertex pair between them, where $\beta \in A_\alpha$ and $\gamma \in A_\delta$. Thus, there are order N^5 non-zero contributions to the variance, each of order N^{-8}/σ^4 . Hence $\text{Var}(\sum_{\alpha \in \mathcal{I}} \xi_\alpha \eta_\alpha)$ is of order N^{-1} , and the overall bound in (25) is of order $N^{-\frac{1}{2}}$. All moment expressions can be bounded explicitly, which makes it possible to compute C numerically. This proves the assertion. \square

C Kernel choice

To calculate IRG-gKSS, we use (7), in (7), $h_{\mathbf{x}}(s, s')$ is the inner product of the Stein operator (5) for the vertex pairs s and s' , calculated using the underlying kernel K and inner product $\langle \cdot, \cdot \rangle$ of the associated RKHS. The test statistic is the average of N^2 values of $h_{\mathbf{x}}(s, s')$ calculated for all pairs of s and s' . To calculate $h_{\mathbf{x}}(s, s')$, we create a list of $N + 1$ networks, the observed network and others by flipping one edge each time and then calculate the graph kernel matrix for this list. Hence, the underlying graph kernel gives the type of signal we are using from our network to calculate $h_{\mathbf{x}}(s, s')$ scores.

Weisfeiler-Lehman kernels For many of our experiments, we use a Weisfeiler-Lehman (WL) kernel, which is based on the Weisfeiler-Lehman graph isomorphism test. It assigns an attribute to each vertex. In our experiments, we use group membership as an initial vertex attribute for WL kernels; for ER graphs, all vertices are labelled as group 1. Iteratively, for each vertex, the attributes of its immediate neighbours are aggregated to compute a new attribute for the target vertex. This relabelling is carried out for h iterations. For each graph G , after h iterations the algorithm has created h related graphs $G = G_0, G_1, \dots, G_h$. For two graphs G and G' , with sequences $G = G_0, G_1, \dots, G_h$ and $G' = G'_0, G'_1, \dots, G'_h$, the WL (subtree) kernel is given by

$$K_{WL}(G, G') = \sum_{\ell=0}^h k(G_\ell, G'_\ell)$$

where $k(G_\ell, G'_\ell)$ is the subtree kernel which counts the common labels in the two graphs G_ℓ and G'_ℓ ; in this instance, h is also referred to as the (subtree) height. This way, the WL kernel compares the local structure in the two networks. With each step of the WL iterations, we incorporate information about the next order neighbourhood of the vertex into its new label. Since WL kernel compares the local structure in the two networks, it proves a reasonable choice to be used in IRG-gKSS for detecting structural anomalies in the network. The K_{WL} values naturally increase with increasing number of iterations h . We observe empirically that the choice of h affects the power of the IRG-gKSS test. As will be detailed later, we find that the WL kernel with $h = 2$ performs better in detecting the presence of cliques (an anomaly in the local structure), while the WL kernel with $h = 3$ performs better in detecting hubs in the network (a more global structure).

While a WL kernel does not directly depend on density, graph density affects the label refinement process, which in turn influences the kernel value. We observe that in dense graphs, the neighbourhood structure can change substantially with each WL iteration. In sparse graphs, in contrast, the labels which the WL algorithm assigns may stabilise quickly, so that there will then be fewer changes in the WL refinement process. Thus, denser graphs often lead to higher feature complexity and better discrimination, while sparse graphs may suffer from label similarity, reducing kernel effectiveness.

Graphlet kernels The Graphlet kernel is based on counts of subgraph patterns (graphlets) of a fixed size in a graph. Motifs based on graphlets are as building blocks of complex networks. Thus, they are a plausible choice for detecting structural anomalies. The time required to compute the graphlet kernel scales exponentially with the size of the considered graphlets and the edge density of the network, making them computationally more expensive than the WL kernel, see Kriege et al. [2020]. Hence, we use a graphlet kernel to illustrate its effectiveness in some of the experiments and use the WL kernel for most of our experiments due to its computational efficiency.

We did not find a uniformly best choice of the kernel to compute IRG-gKSS and recommend using more than one kernel when testing the fit of a network. However, we do not use the vertex-edge histogram kernel to compute IRG-gKSS. The vertex-edge histogram kernel only signals the structural similarities of the vertex and edge labels of the networks compared, counting how many times each label (vertex and edge) appears in both networks and how many of those common labels are shared (Kriege et al. [2020]). In our implementation, we assume that the number of vertices and labels are known a priori; the only signal we get from using the vertex-edge histogram kernel is the density of edges of each type. In this case, the test detects the lack of fit only if the edge density is different in the observed network from the hypothesised model, with the only advantage of being faster to calculate than other graph kernels.

D Computational complexity

The computation time of IRG-gKSS² depends on the size n of the network and the computational complexity of the underlying graph kernel. To compute a single value of IRG-gKSS², the algorithm computes the kernel matrix for a list of $\binom{n}{2} + 1$ networks of size n and uses it to calculate a value of the final test statistic in a way that requires some simple matrix operations in R. A full test requires computing an IRG-gKSS² for the observed network and a set of IRG-gKSS² for all M simulated networks under the null model. For the estimated IRG-gKSS² with edge-resampling (using B edge indicators instead of the full set of all possible edge indicators), the list of networks for which we need to compute the kernel matrix reduces to $B + 1$.

Figure 3 shows the executing time (in seconds) for ER graphs with $p = 0.06$ and varying size, using the WL kernel with height $h = 3$ on a system with an Intel Core i7-8700, 32 GB DDR4-2666 RAM, and Windows 11 Enterprise using R 4.5.0. The scaling with respect to size is almost linear, whereas the scaling with respect to M , the number of simulated networks, is almost quadratic, reflecting that $\binom{M}{2}$ network comparisons are carried out.

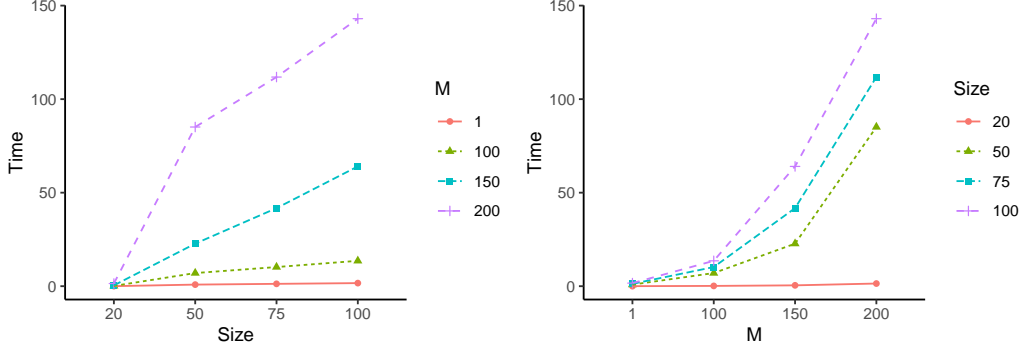


Figure 3: Execution time to calculate IRG-gKSS, using the WL kernel with $h = 3$, for networks simulated from corresponding $ER(n, 0.06)$ models. Left: dependence on size n , for different numbers M of simulated networks; right: dependence on M , for different sizes n .

Code details For simulating networks, we use a similar implementation as in the GoodFitSBM (0.0.1) R package. For graph kernels in R we use the graphkernel (1.6.1) package. The code to compute IRG-gKSS from the kernels extends the code of Xu and Reinert [2021]. The code also uses the R libraries Matrix and HelpersMG. For the graphlet kernel, we also use grakel version 0.1.8 from Python. The code is available at the anonymous GitHub site IRG-gKSS.

E Additional details and results for synthetic experiments

This section gives further details of the synthetic experiments from the main paper, as well as some additional results. All tests are carried out at the 5% level.

E.1 Experiment 1: Planted hubs

As mentioned in Section 4.1.1 of the main text, Experiment 1 is based on two choices, R and k , and different network models. We denote by $s_d = s_d(G)$ the standard deviation of the vector of degrees in a network G . We repeatedly simulate a network G from an $ERMM(\mathbf{n}, \mathbf{Q})$ model, attempt to plant R hubs in these networks which increase the largest degree by ks_d without disturbing the edge density of the original network, using Algorithms 3 and 4, and test the fit of the $ERMM(\mathbf{n}, \mathbf{Q})$ model on these networks with planted hubs.

For the simulations, we choose $n = 50$. In Section 4.1.1, results are given for a two-group $ERMM$ with an even split between the groups and a probability matrix

$$\mathbf{Q} = \begin{pmatrix} 0.20 & 0.01 \\ 0.01 & 0.20 \end{pmatrix} \quad (26)$$

resulting in the within-group subgraphs being fairly dense, and the between-group subgraphs being fairly sparse. We also give results for an unbalanced split in addition to the equal split, given by

$$\mathbf{n}_{ub} = (10, 40), \quad \text{and} \quad \mathbf{n} = (25, 25). \quad (27)$$

To assess the effect of the height h in the WL kernel in this setting, we carry out this experiment using WL kernels with both $h = 2$ and $h = 3$. For the planted hubs, the IRG-gKSS tests computed using the WL kernel with $h = 3$, from $ERMM$ networks with equal split in two groups, have slightly

Algorithm 3 Iterative Planted Hubs Construction

Input: G : Input graph with n vertices,
 R : Number of hub planting attempts,
 k : Scaling factor for maximum degree increase,
 C : A numeric vector of vertex group labels.
Output: A modified graph G_{hubs} with up to R planted hubs
Initialize:
 $G_{hubs} = G$ (copy of the original graph)
 Get $\mathbf{d} = (d_0, \dots, d_{n-1})$, the vector with entry d_ℓ the degree of vertex ℓ in G
 Set $d_m = \max(\mathbf{d})$ (starting from a vertex with maximum degree)
 Set iteration counter $i = 1$
while $d_m \neq \text{NA}$ && $i \leq R$ **do**
 Apply Algorithm 4 (planting a hub) to G_h using, k , and C from input and current d_m
 Update G_{hubs} with the modified graph
 Increment $i = i + 1$
 Recompute the updated degree vector \mathbf{d} from the updated graph G_{hubs}
 Sort the entries of the updated \mathbf{d} in descending order
 Set d_m to equal the i -th largest unique degree
end while
return the modified graph G_{hubs}

higher power than the IRG-gKSS tests using the WL kernel with $h = 2$, see Figures 1 and 4. In contrast, for ERMM networks with an unbalanced split in two groups, the IRG-gKSS tests computed using the WL kernel with $h = 2$ have higher power than the IRG-gKSS tests using the WL kernel with $h = 3$, as illustrated in Figures 5 and 6.

Illustrating this discrepancy further, for a network simulated from the ERMM(\mathbf{n}, \mathbf{Q}) model with $\mathbf{n} = (15, 15)$ and \mathbf{Q} given in (26) and a corresponding network with planted hubs, given in Figure 7, the IRG-gKSS test rejects the fit of the ERMM(\mathbf{n}, \mathbf{Q}) model for the network with planted hubs when using the WL kernel with $h = 3$, but it does not reject the fit when using the WL kernel with $h = 2$. The heatmap plots for the $h(s, s')$ matrix in (7) of the main text (the inner product of the Stein operator for all possible pairs of edge indicators) are given in Figures 8 and 9. The discrepancy between the matrix under the null hypothesis and under the planted hub alternative is more pronounced when using $h = 3$ compared to $h = 2$. One could think of a hub as being a global structure, for which a larger h in a WL kernel could be more appropriate. We also conclude that this example shows that there is no clear choice about which h to employ; the choice of h should be informed by the nature of the alternative hypothesis.

E.2 Experiment 2: A planted clique

In the next experiment, we simulate a network from an ERMM(\mathbf{n}, \mathbf{Q}) model, move its existing edges to plant a clique of size K , if possible, keeping the number of edges of each type as of the original simulated network, if possible, and test the fit of the ERMM(\mathbf{n}, \mathbf{Q}) to the transformed network with the planted clique. Similarly to the planted hub example, if planting a clique is not possible, we discard that network and simulate a new network to plant the clique; we also record the frequency with which this happens. By planting a clique, we tamper with the structure of the network while keeping the edge density of each edge type constant. Thus, the model ERMM(\mathbf{n}, \mathbf{Q}) is misspecified for the resulting network with a planted clique. For the figures in this subsection, the numbers inside the boxes in the plots are the total number of networks in $m = 50$ samples from an ER(n, p) that had the number of edges less than $\binom{K}{2}$ to plant a clique of size K and were, therefore, not used in the experiment. The number $m = 50$ is the number of repetitions of the goodness-of-fit test. We repeat the goodness of fit test for 50 simulated networks with a planted clique of size K , while using the set of $M = 200$ IRG-gKSS values calculated from M networks simulated from the ERMM(\mathbf{n}, \mathbf{Q}) model.

In addition to Figure 2 in the main paper, here we give results for more parameter settings. Figures 10 and 11 illustrate the power of the edge resampling version compared to the version without edge resampling of the IRG-gKSS test to test the fit of ER($50, p$) models using the WL kernel with $h = 2$,

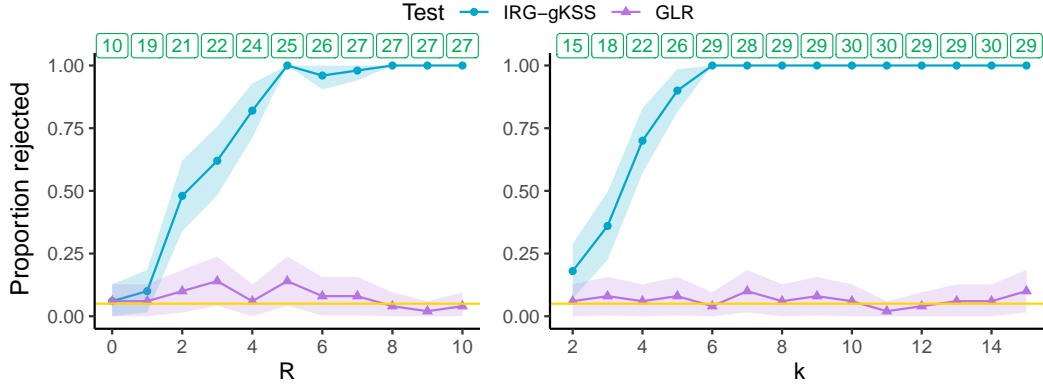


Figure 4: Power of the tests for the fit of an $\text{ERM}(\mathbf{n}, \mathbf{Q})$ model to a network of size 50 with planted hubs, with \mathbf{n} from (27) and \mathbf{Q} from (26). The numbers in the boxes at the top of the plot are the average maximum degree observed in $m = 50$ repetitions of the test for each setting on the x -axis. For the figure on the left side, we fix $k = 4$ and let R vary, and in the right side figure, we fix $R = 3$ and let k vary. For this experiment, we use a WL kernel with $h = 2$.

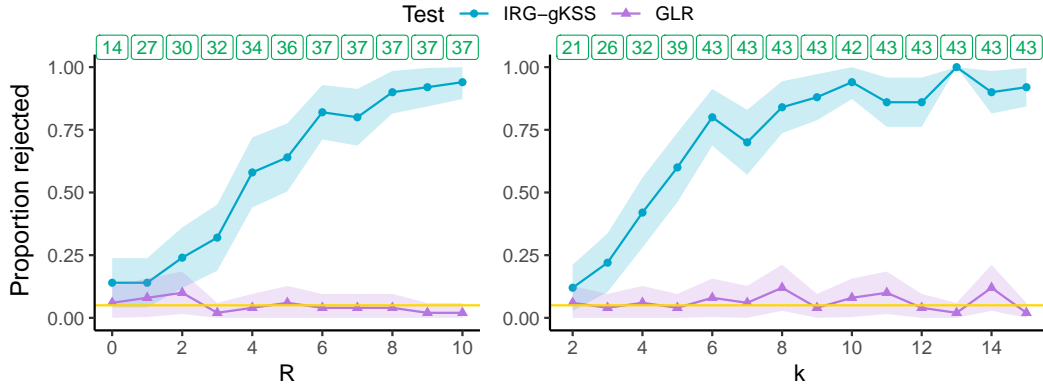


Figure 5: Power of the tests for the fit of an $\text{ERM}(\mathbf{n}_{ub}, \mathbf{Q})$ model to a network of size 50 with planted hubs, with \mathbf{n}_{ub} from (27) and \mathbf{Q} from (26). The numbers in the boxes at the top of the plot are the average maximum degree observed in $m = 50$ repetitions of the test for each setting on the x -axis. For the figure on the left side, we fix $k = 4$ and let R vary, and in the right side figure, we fix $R = 3$ and let k vary. For this experiment, we use a WL kernel with $h = 3$.

Algorithm 4 Planting a hub in a simulated network

Input: G : Input graph,
 d_m : Initial degree of the hub vertex
 k : Scaling factor for maximum degree increase,
 C : A numeric vector of vertex group labels.
Output: A modified graph G_{hub} with a "planted hub" (or original G if no hub planting is possible).
Compute vertex degrees and standard deviation:
 Get \mathbf{d} , the vector with entry d_ℓ the degree of vertex ℓ in G
 Compute s_d , the standard deviation of the vector \mathbf{d}
Identify hub candidate:
 Set u_{hub} , the first vertex in the vertex list of graph G with degree exactly d_m
Set the number of new neighbours for u_{hub} :
 Get $d^* = \max(1, \lceil k * s_d \rceil)$
 Set $n_{new_nei} = d^* - d_{u_{hub}}$, where $d_{u_{hub}}$ is the degree of u_{hub}
Find the potential additional neighbour set $target_V$ for u_{hub} :
 $target_V = V(G)$ excluding the current neighbours of u_{hub} and u_{hub} itself
 if $d^* = d_{u_{hub}}$ **or** $target_V$ is empty **then** return G (in this case no hub planting is possible)
Filter $target_V$ by a group membership constraint:
 For each v in $target_V$, keep v if at least one neighbour of v has the group membership of u_{hub}
 Store these in $filtered_targets$
 if $filtered_targets$ is empty **then** return G (in this case no hub planting is possible)
Sample potential neighbours to add:
 if $length(filtered_targets) \leq n_{new_nei}$ **then** set $pot_nei = filtered_targets$
 else randomly sample n_{new_nei} vertices from $filtered_targets$ and store in pot_nei
 end if
Prepare for edge replacement:
 Initialize empty vectors to_del and new_nei
 for v in pot_nei **do**
 Get neighbors of v of the same type as u_{hub} and store in N_v
 if N_v is empty **then** skip to next v
 else Sample a neighbour del_vertex from N_v to disconnect with v
 Concatenate the pair (v, del_vertex) with to_del vector
 Check whether the resulting vector (to_del), does not contain duplicate pairs (edges)
 If it does: resample the neighbour to delete until the resulting vector does not contain
 duplicate pairs; if no such neighbour can be found: drop v and move to the next candidate
 in pot_nei
 Add v to new_nei
 end if
 end for
Post-processing edge list:
 if to_del is empty or does not match expected size ($2 * length(new_nei)$) **then** return G
Apply graph edits:
 Delete the edges in to_del from G
 Add an edge between u_{hub} and each vertex in new_nei
return the modified graph G_{hub}

for different p . We repeat this experiment for networks of size 100; the results are shown in Figure 15. These figures illustrate the power of the IRG-gKSS test to detect discrepancies from the null model in the presence of a clique in the network, with the minimum size of the clique detected by the test depending on the edge density of the network. As the expected degree of a vertex in an $ER(n, p)$ network is $(n - 1)p$, we see that cliques can be detected even if they are only slightly larger than the expected degree. The GLR test does not detect the difference.

To illustrate further, we repeat this experiment for ERMMS with four different parameter settings using two different settings for \mathbf{Q} given by

$$\mathbf{Q}_{01} = \begin{pmatrix} 0.20 & 0.01 \\ 0.01 & 0.20 \end{pmatrix} \quad \text{and} \quad \mathbf{Q}_{02} = \begin{pmatrix} 0.6 & 0.1 \\ 0.1 & 0.6 \end{pmatrix}, \quad (28)$$

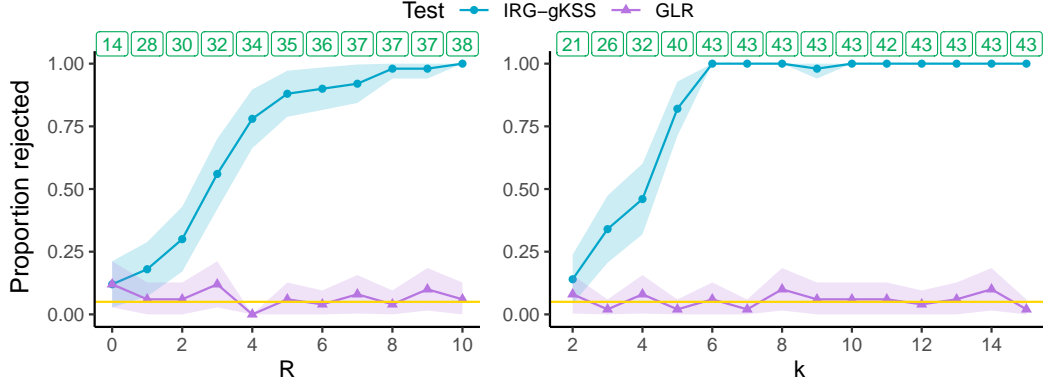


Figure 6: Power of the tests for the fit of an $\text{ERMM}(\mathbf{n}_{ub}, \mathbf{Q})$ model to the network of size 50 with planted hubs, with \mathbf{n}_{ub} from (27) and \mathbf{Q} from (26). The numbers in the boxes at the top of the plot are the average maximum degree observed in $m = 50$ repetitions of the test for each setting on the x-axis. For the figure on the left side, we fix $k = 4$ and let R vary, and in the right side figure, we fix $R = 3$ and let k vary. For this experiment, we use a WL kernel with $h = 2$.

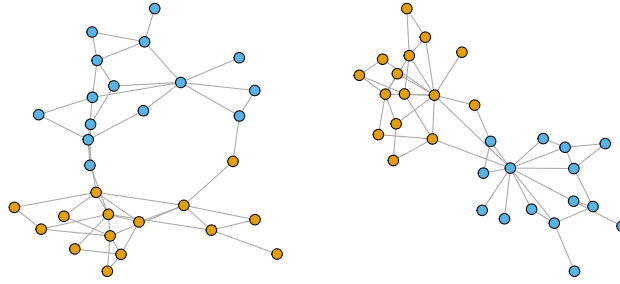


Figure 7: Simulated networks simulated from Left: an $\text{ERMM}((15, 15), \mathbf{Q})$ model with \mathbf{Q} as in (26); right: starting from the same network, the network with planted hubs using $R = 2$ and $k = 2$.

and the two settings for \mathbf{n} from (27). The results in Figure 16 illustrate the power of the IRG-gKSS test to detect the presence of a clique in the network, depending on the size of the clique, the density of the network, and the type of split.

To assess the effect of the height h in the WL kernel in this setting, we use WL kernels with $h = 2$, $h = 3$, $h = 5$ and $h = 7$ for the IRG-gKSS test to test the fit of the $\text{ER}(50, 0.02)$ model on networks with a planted clique and observed that in this setting, increase in the height h in the WL kernel cause the IRG-gKSS test to only detect the presence of a larger size clique, see Figure 17. We also used the graphlet kernel with two different graphlet sizes $k = 3$ and $k = 5$ for the planted clique experiment. With results given in Figure 18, we do not see a substantial improvement in the power of the test despite these kernels being much more expensive to calculate.

To further explore the effect of the choice of h on the IRG-gKSS test, we simulate a network from the $\text{ER}(20, 0.06)$ model and plant a clique of size 5; an example is shown in Figure 12. The IRG-gKSS test rejects the fit of the $\text{ER}(20, 0.06)$ model for the network with a planted clique when using the WL kernel with $h = 2$, but it does not reject the fit when using the WL kernel with $h = 3$. The heatmap plots for the $h(s, s')$ matrix in (7), in Figures 13 and 14, illustrate how this discrepancy arises. For $h = 2$, the difference between the matrices is more pronounced, as this setting captures the direct neighbourhood of vertices and their immediate neighbours. Larger values of h , however, attenuate these differences by incorporating similarities in extended neighbourhoods. Notably, cliques and non-cliques become harder to distinguish at higher h because their multi-hop neighbourhood structures become more similar, obscuring local distinctions.



Figure 8: Heatmap plot of $h(s, s')$ matrix from left: Original network simulated from an $\text{ERMM}((15, 15), \mathbf{Q})$ model; right: the network with planted hubs using $R = 2$ and $k = 2$. For this plot, we use WL with $h = 2$.

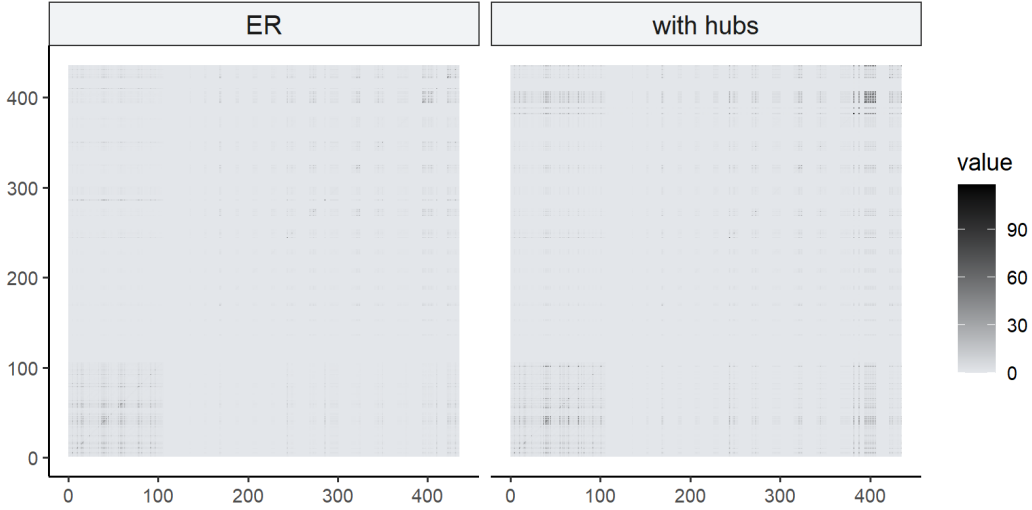


Figure 9: Heatmap plot of $h(s, s')$ matrix from left: Original network simulated from an $\text{ERMM}((15, 15), \mathbf{Q})$ model; right: the network with planted hubs using $R = 2$ and $k = 2$. For this plot, we use WL with $h = 3$.

E.3 Experiment: Networks simulated from a non-linear preferential attachment model

Here is an additional experiment not mentioned in the main text. In this experiment, we simulate networks on 50 vertices from a non-linear preferential attachment (NLPA) model with different parameter settings and test the fit of a relevant $\text{ER}(n, p)$ model on these simulated networks. The algorithm to simulate a network under an $\text{NLPA}(m, \alpha)$ model starts with an initial network with $m_0 \geq m$ vertices. At each step, we add a vertex, and sample m distinct vertices from the existing

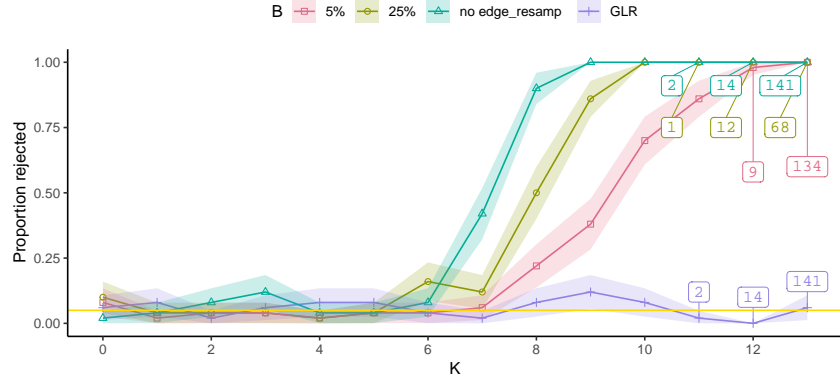


Figure 10: Power of the tests for the fit of an $ER(50, 0.06)$ model to a network of size 50 with a planted clique, using edge resampling and the without-edge-resampling version of IRG-gKSS. For this experiment, we use a WL kernel with $h = 2$. The numbers in the boxes are the total number of networks, out of $m = 50$ networks, sampled from the $ER(50, 0.06)$ model that fewer than $\binom{K}{2}$ so that it was not possible to plant a clique of size K without disturbing the density and were, therefore, not used in the experiment. For this experiment, we use a WL kernel with $h = 2$.

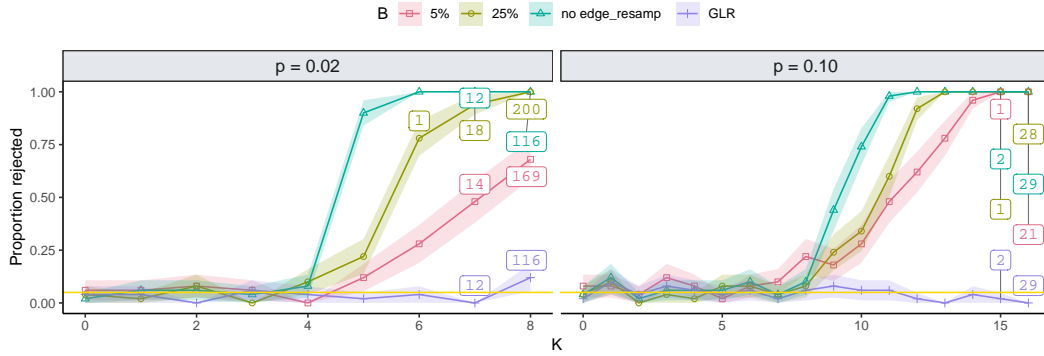


Figure 11: Power of the tests for the fit of an $ER(50, p)$ model to a network of size 50 with a planted clique, using edge resampling and the without-edge-resampling version of IRG-gKSS. For this experiment, we use a WL kernel with $h = 2$.

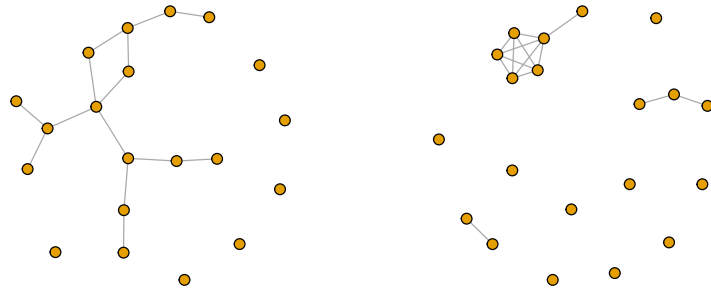


Figure 12: Simulated networks simulated from Left: $ER(20, 0.06)$ model; right: starting from the same network, the network with a planted clique of size $K = 5$.

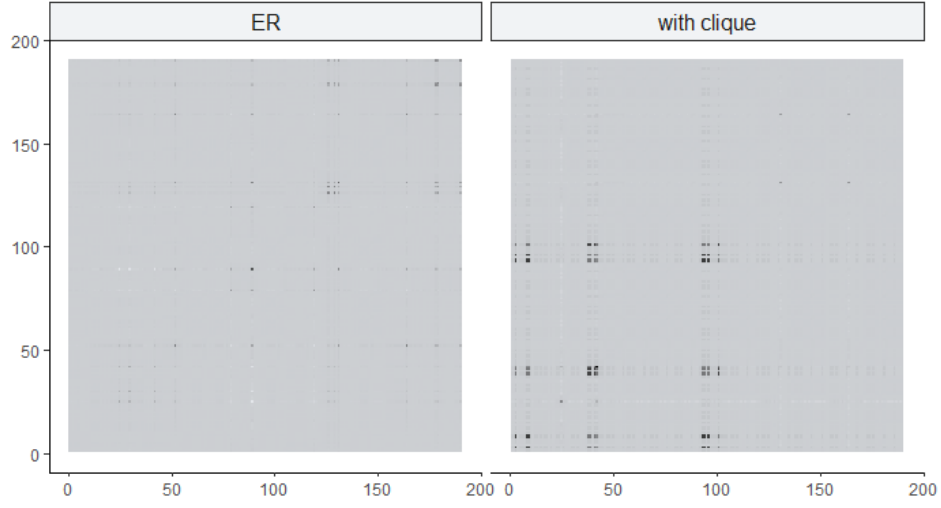


Figure 13: Heatmap plot of $h(s, s')$ matrix from left: Original network simulated from an $ER(20, 0.06)$ model; right: the network with planted clique of size $K = 5$. For this plot, we use WL with $h = 2$.

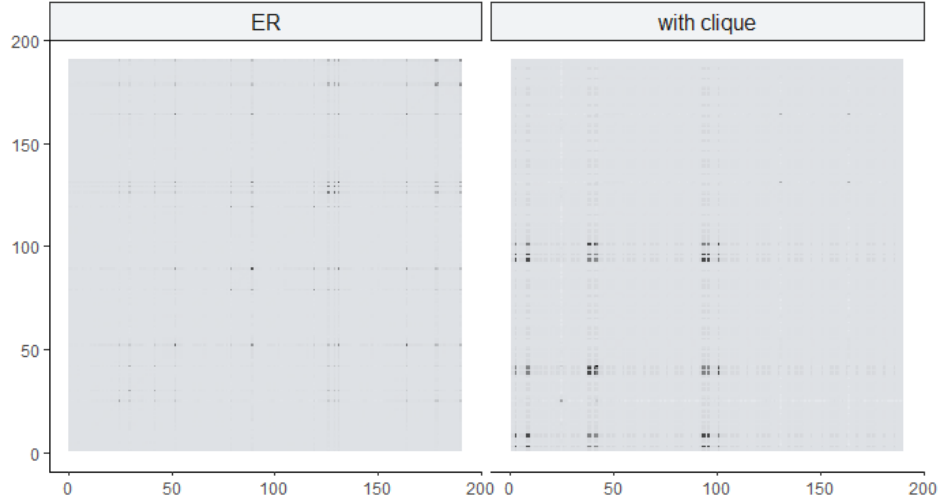


Figure 14: Heatmap plot of $h(s, s')$ matrix from left: Original network simulated from an $ER(20, 0.06)$ model; right: the network with planted clique of size $K = 5$. For this plot, we use WL with $h = 3$.

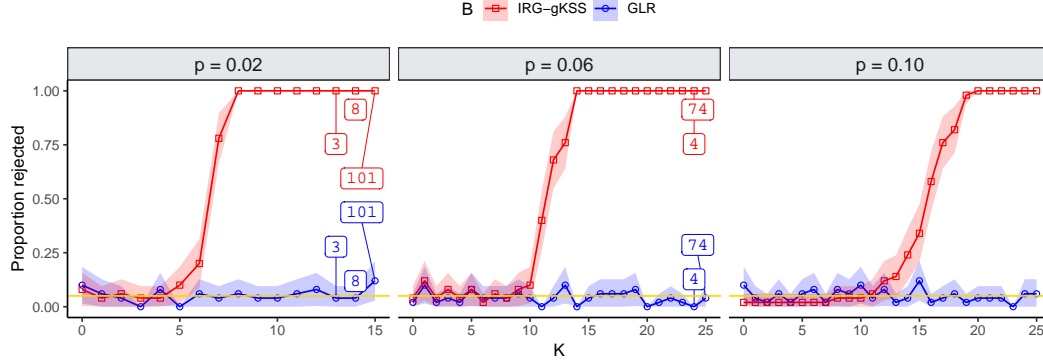


Figure 15: Power of the tests for the fit of an $ER(100, p)$ model to a network with a planted clique of size K . For this experiment, we use a WL kernel with $h = 2$.

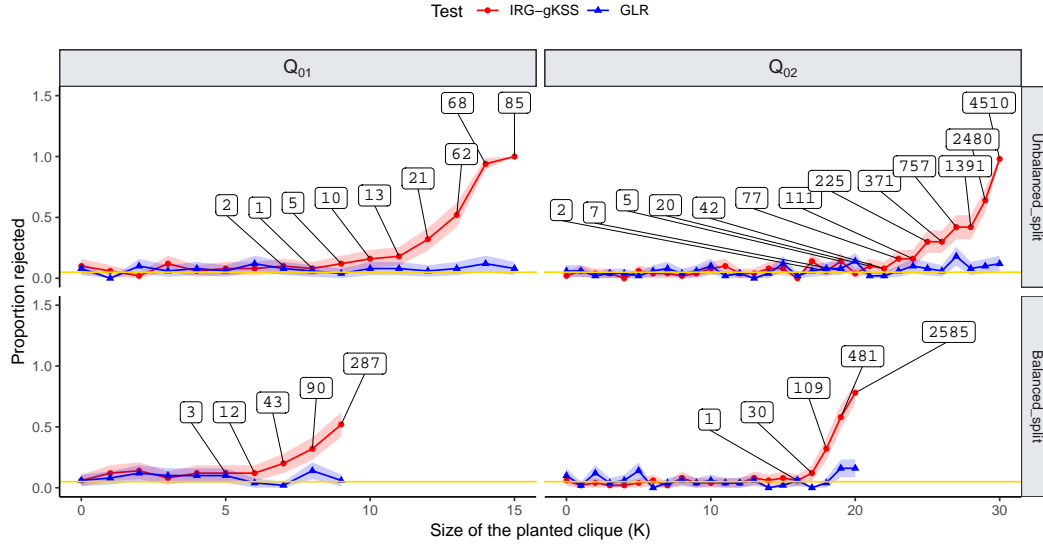


Figure 16: Power of the tests for the fit of an $ERM(n, Q)$ with n from (27) and Q from (26) to the network with a planted clique. For this experiment, we use a WL kernel with $h = 2$.

vertices in the network, sampling vertex i with probability

$$p_i = \frac{k_i^\alpha}{\sum_j k_j^\alpha}.$$

Here k_i is the degree of vertex i at the current step, and the sum is over all pre-existing vertices j (so that the denominator results in twice the current number of edges in the network). If vertex i is sampled, then an edge between the new vertex and vertex i is created. The process continues until we have a network with n vertices. We use the `sample_pa` function from the *igraph* library in R to simulate these networks. The resulting networks are different from ER networks through their construction; edge indicators are not independent, and in particular, for large networks, one would anticipate to see more vertices with large degrees. Figure 19 shows some instances of this model on 50 vertices and different parameter settings.

The results in Table 4 give the proportion of times that the IRG-gKSS test at level 5% rejected the fit of an $ER(n, p)$ model to a network simulated from an $NLPA(m, \alpha)$ model in 50 repetitions. We used

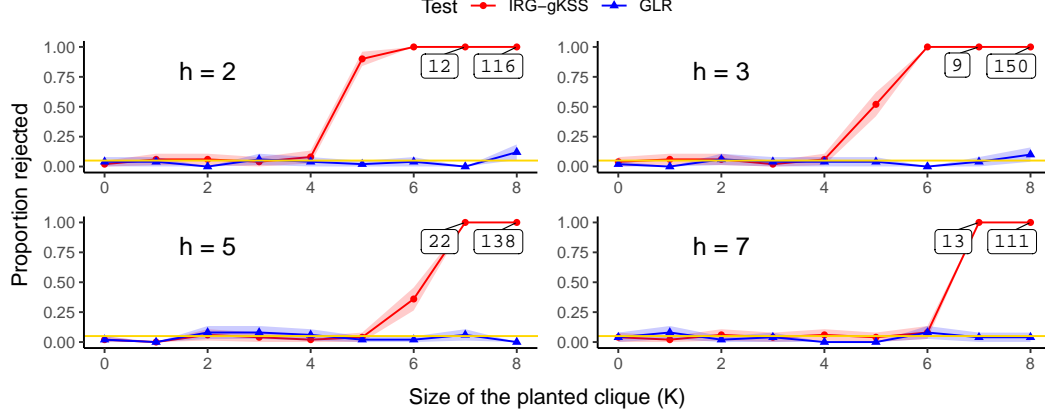


Figure 17: Power of the tests for the fit of an $ER(50, 0.02)$ model to a network with a planted clique of size K using WL kernels with different subtree heights h .

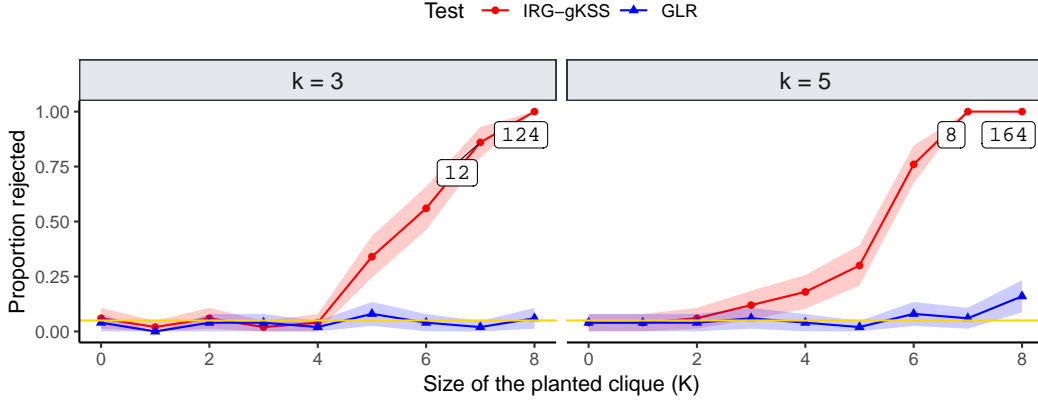


Figure 18: Power of the tests for the fit of an $ER(50, 0.02)$ model to the network with a planted clique. For this experiment, we use the graphlet kernel with $k = 3$ and 5 .

IRG-gKSS with three kernels, namely the WL kernel with $h = 2$, the WL kernel with $h = 3$ and the normalised graphlet kernel with $k = 3$, and record their results separately in Table 4.

We find that for large n the difference to an ER model is clearly detected. For small n , only some instances are deemed by the test to be clearly different from an ER model. For the WL kernels, the difference is easier to detect for $m = 1$ compared to $m = 2$. In contrast, for the graphlet kernel, the difference is easier to detect for $m = 2$ compared to $m = 1$. In particular, none of the kernels has uniformly more power than the other kernels.

E.4 Experiment: Testing the fit of an ERMM

When testing within a parametric model family, a (generalised) likelihood ratio test (LRT) is usually most powerful, see for example Zeitouni et al. [1992]. How much less powerful is an IRG-gKSS test? To assess this question, in this experiment, which complements those in the main text, we test the fit of an $ERMM(\mathbf{n}, \mathbf{Q}_0)$ to a network simulated from an $ERMM(\mathbf{n}, \mathbf{Q}_1)$ using Algorithms 1 and 2 and a likelihood ratio test (LRT). More specifically, we simulate networks of size 50 from an $ERMM(\mathbf{n}, \mathbf{Q}_1)$ with two groups, where the within-block probabilities are identical but the between-block probabilities

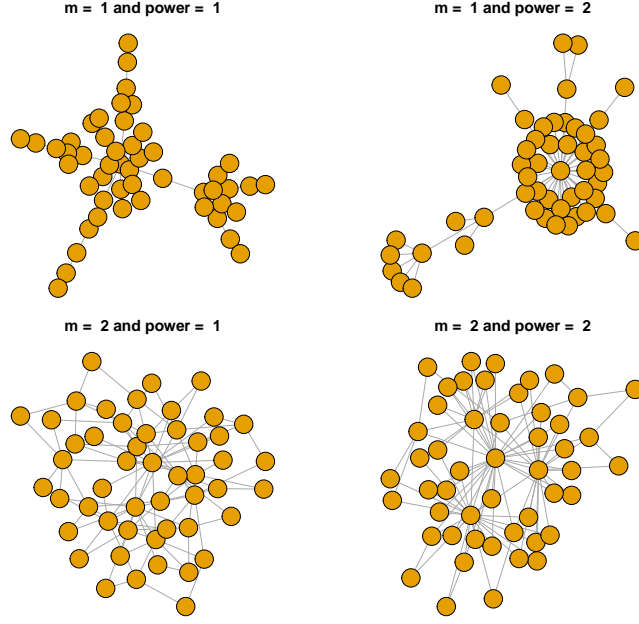


Figure 19: Networks on 50 vertices created from an NLPA model with different parameter settings.

Table 4: Testing the fit of the ER model on a network simulated from a preferential attachment model

| Model Parameters | | | Proportion rejected | | |
|------------------|--------------|---------|---------------------|-----------------|-----------------------|
| | | | WL with $h = 2$ | WL with $h = 3$ | Graphlet with $k = 3$ |
| $n = 20$ | $\alpha = 1$ | $m = 1$ | 0.38 | 0.44 | 0.10 |
| | | $m = 2$ | 0.02 | 0.04 | 0.30 |
| | $\alpha = 2$ | $m = 1$ | 0.94 | 0.96 | 0.90 |
| | | $m = 2$ | 0.76 | 0.88 | 1.00 |
| $n = 50$ | $\alpha = 1$ | $m = 1$ | 0.88 | 0.74 | 0.14 |
| | | $m = 2$ | 0.62 | 0.20 | 0.96 |
| | $\alpha = 2$ | $m = 1$ | 1.00 | 1.00 | 1.00 |
| | | $m = 2$ | 1.00 | 1.00 | 1.00 |
| $n = 100$ | $\alpha = 1$ | $m = 1$ | 1.00 | 0.98 | 0.14 |
| | | $m = 2$ | 1.00 | 0.88 | 0.98 |
| | $\alpha = 2$ | $m = 1$ | 1.00 | 1.00 | 1.00 |
| | | $m = 2$ | 1.00 | 1.00 | 1.00 |

are different. We use following setting for \mathbf{Q}_0 and \mathbf{Q}_1 ;

$$\mathbf{Q}_{01} = \begin{pmatrix} 0.20 & 0.01 \\ 0.01 & 0.20 \end{pmatrix} \quad \text{and} \quad \mathbf{Q}_{02} = \begin{pmatrix} 0.6 & 0.1 \\ 0.1 & 0.6 \end{pmatrix},$$

and

$$\mathbf{Q}_{11} = \begin{pmatrix} 0.20 & Q_{12} \\ Q_{12} & 0.20 \end{pmatrix} \quad \text{and} \quad \mathbf{Q}_{12} = \begin{pmatrix} 0.6 & Q_{12} \\ Q_{12} & 0.6 \end{pmatrix}, \quad (29)$$

with Q_{12} a parameter. We use unbalanced (ub) and balanced group splits given by $\mathbf{n}_{ub} = (10, 40)$ and $\mathbf{n} = (25, 25)$ as in (27).

We compare the IRG-gKSS test, without and with edge resampling, using a WL kernel with height $h = 3$, to the likelihood ratio (LR) test, for which we specify the parameters in the alternative model as given in (27) and (29). Figure 20 shows the proportion of tests that reject the null model at level 5%. For the test with edge-resampling using Algorithm 2, we repeat the test for different values of B

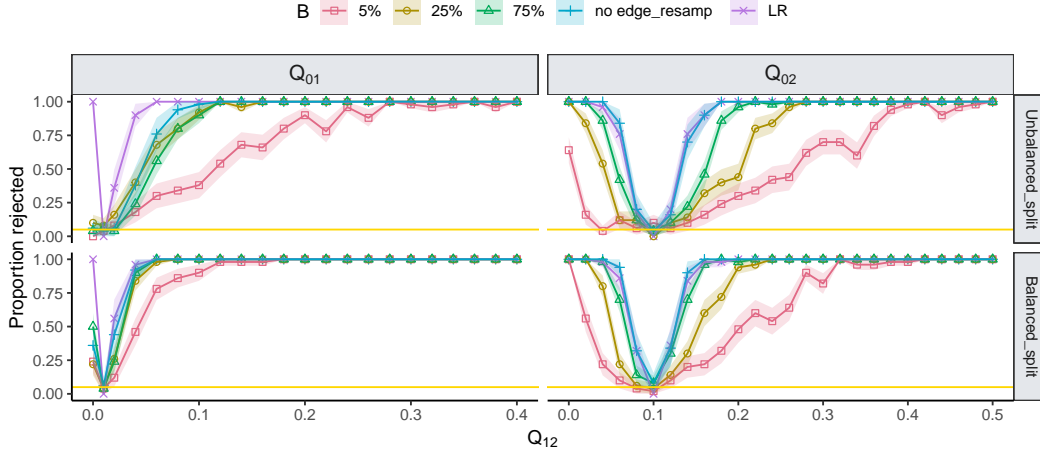


Figure 20: Power of the test at level 5% for the fit of an $\text{ERMM}(\mathbf{n}, \mathbf{Q})$, with \mathbf{n} and \mathbf{Q} from (27) and (28), to 50 networks simulated from an $\text{ERMM}(\mathbf{n}, \mathbf{Q})$ model, with \mathbf{n} and \mathbf{Q} from (27) and (29), using a WL kernel with $h = 3$. The yellow line indicates the significance level (0.05).

in the test statistic (9). In Figure 20, the values of B are reported as a proportion of $N = \binom{n}{2}$, the number of possible edges in the network of size n .

From Figure 20, we observe that the power of IRG-gKSS is lower than that of the LR test, which is supposed to perform best in this experimental setting, but not by a large margin. Also, with edge-resampling, IRG-gKSS performs reasonably well even when sampling only 25% of the vertex pairs. Moreover, in the sparse network setting, using as few as 5% of the vertex pairs still gives a test with some power.

F Real Data Applications

F.1 Parameter estimation

For the real data applications, the model parameters have to be estimated. For ERMM models with given group labels, the standard maximum likelihood estimators are used. When the group assignments are not given, but the number of groups is suggested, then we employ the Louvain algorithm Blondel et al. [2008] to obtain the group assignments. This algorithm assigns vertices to communities based on modularity as a quality measure of a partition. As this algorithm is random, we run it 100 times and select the partition with the highest modularity.

For the DCSBM, we estimate the parameters using the ‘DCSBM.estimate’ function from the `randnet` package in R. This package fits a Poissonized DCSBM to the data, as is customary. Here we use these parameter estimates to take $p_{u,v} = 1 - e^{-Q_{g_u, g_v} \theta_u \theta_v}$ for all u and v in the network as parameters in the null model to test the fit of a DCSBM.

F.2 Lazega’s lawyers networks

The collection of Lazega’s lawyers networks [Lazega, 2001] is constructed from a data set collecting results of a study on relationships between 71 attorneys (partners and associates) of a Northeastern US corporate law firm, during 1988-1991.

The data set includes (among others) information on work relationships, advice relationships, and friendship relationships among the 71 attorneys. From this data set, several undirected networks are constructed, with lawyers represented by vertices. In the *work network*, two vertices are connected by an edge if the two lawyers have spent time together on at least one case, or have been assigned to the same case, or either of them has read or used a work product created by the other. In the *advice network*, an edge represents that they consult each other for basic professional advice for their work,

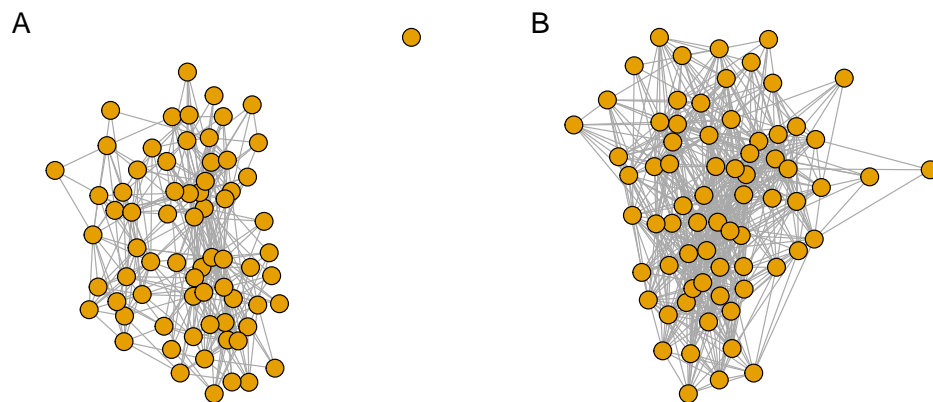


Figure 21: Lazega's lawyers networks: (A) work, (B) advice.

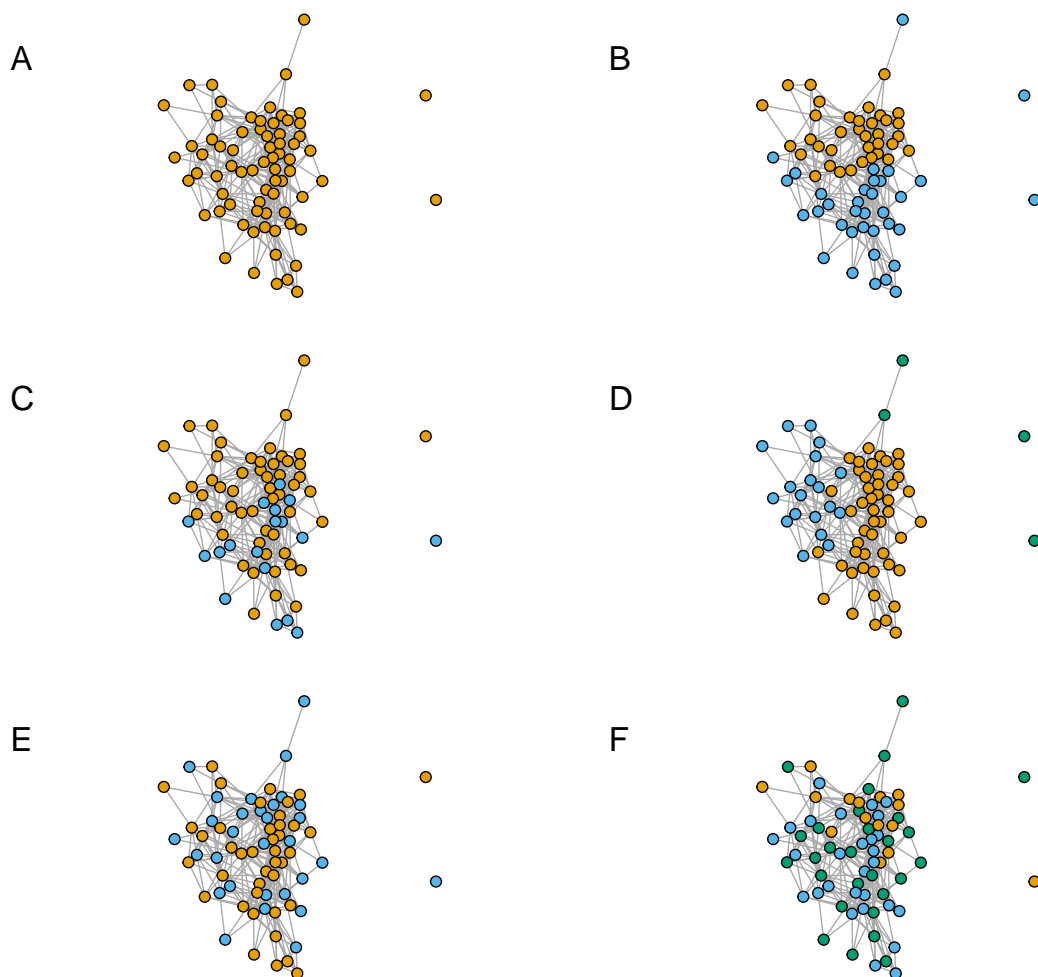


Figure 22: Lazega's lawyers' friendship network with vertices coloured according to (A) Single group, (B) Status (Orange: partner; Blue: associate), (C) Gender (Orange: male; Blue: female), (D) Office (Orange: Boston; Blue: Hartford; Green: Providence), (E) Practice (Orange: litigation; Blue: corporate), and (F) Law school (Orange: Harvard, Yale; Blue: UCon; Green: other).

and an edge in the *friendship network* indicates that the two lawyers socialise with each other outside work.

Various attributes of the lawyers are also part of the dataset, such as seniority, formal status, office in which they work, gender, law school attended, individual performance measurements (hours worked, fees brought in), and attitudes concerning various management policy options. The ethnography, organisational, and network analyses of this data set are available in Lazega (2001).

For each of these networks, we create groups according to different attributes. The parameter estimates of these networks that we use as parameters of the null model, and the IRG-gKSS test results at 5% level, are as follows.

1. For the work network, we propose an ER model with $n = 71$ and $p = 0.152$. For this model, the IRG-gKSS test does not reject the fit.
2. For the advice network, we propose an ER model with $n = 71$ and $p = 0.2885$. For this model, the IRG-gKSS test does not reject the fit.
3. For the friendship network, the situation is more complex. First, we test the fit of an ER model with $n = 71$ and $p = 0.1605634$; IRG-gKSS rejects the fit of this model. Thus, there is a need for a more complex model. We therefore test the fit of different ERMMs and DCSBMs depending upon groups created according to different vertex attributes, as follows.

(a) **Status.** For groups created according to status, we test an ERMM with

$$\mathbf{n} = (36, 35) \text{ and } \mathbf{Q} = \begin{pmatrix} 0.2968 & 0.0730 \\ 0.0730 & 0.2017 \end{pmatrix}.$$

For a corresponding DCSBM we use

$$\mathbf{n} = (36, 35), \quad \mathbf{Q} = \begin{pmatrix} 374 & 92 \\ 92 & 240 \end{pmatrix}$$

and

$$\boldsymbol{\theta} = (0.0172, 0.0215, 0.0086, 0.0472, 0.0129, 0.0043, 0.0064, 0.0150, 0.0300, 0.0300, 0.0300, 0.0472, 0.0515, 0.0193, 0.0086, 0.0279, 0.0536, 0.0193, 0.0129, 0.0300, 0.0322, 0.0236, 0.0150, 0.0536, 0.0322, 0.0515, 0.0408, 0.0279, 0.0279, 0.0172, 0.0601, 0.0150, 0.0279, 0.0258, 0.0279, 0.0279, 0.0030, 0.0452, 0.0452, 0.0392, 0.0602, 0.0482, 0.0542, 0.0000, 0.0241, 0.0181, 0.0000, 0.0211, 0.0181, 0.0271, 0.0241, 0.0422, 0.0090, 0.0361, 0.0090, 0.0361, 0.0452, 0.0422, 0.0181, 0.0241, 0.0090, 0.0151, 0.0060, 0.0633, 0.0693, 0.0482, 0.0151, 0.0271, 0.0181, 0.0211, 0.0181).$$

(b) **Gender.** For groups created according to gender, we test an ERMM with

$$\mathbf{n} = (53, 18) \text{ and } \mathbf{Q} = \begin{pmatrix} 0.1821 & 0.1184 \\ 0.1184 & 0.2287 \end{pmatrix}.$$

For a corresponding DCSBM we use

$$\mathbf{n} = (53, 18), \quad \mathbf{Q} = \begin{pmatrix} 502.001 & 113.001 \\ 113.001 & 70.001 \end{pmatrix}$$

and

$$\boldsymbol{\theta} = (0.0130, 0.0163, 0.0065, 0.0358, 0.0098, 0.0033, 0.0049, 0.0114, 0.0228, 0.0228, 0.0228, 0.0358, 0.0390, 0.0146, 0.0065, 0.0211, 0.0407, 0.0146, 0.0098, 0.0228, 0.0244, 0.0179, 0.0114, 0.0407, 0.0244, 0.0390, 0.1038, 0.0211, 0.0710, 0.0130, 0.0455, 0.0114, 0.0211, 0.0656, 0.0211, 0.0211, 0.0016, 0.0820, 0.0820, 0.0211, 0.0325, 0.0260, 0.0984, 0.0000, 0.0130, 0.0328, 0.0000, 0.0383, 0.0098, 0.0146, 0.0437, 0.0228, 0.0049, 0.019, 50.0049, 0.0195, 0.0820, 0.0228, 0.0328, 0.0437, 0.0164, 0.0081, 0.0033, 0.1148, 0.0374, 0.0260, 0.0273, 0.0146, 0.0328, 0.0114, 0.0328).$$

(c) **Office.** For groups created according to office, we test an ERMM with

$$\mathbf{n} = (48, 19, 4) \text{ and } \mathbf{Q} = \begin{pmatrix} 0.2464 & 0.0647 & 0.0156 \\ 0.0647 & 0.3391 & 0.0000 \\ 0.0156 & 0.0000 & 0.1666 \end{pmatrix}.$$

For a corresponding DCSBM we use

$$\mathbf{n} = (48, 19, 4), \quad \mathbf{Q} = \begin{pmatrix} 556.001 & 59.001 & 3.001 \\ 59.001 & 116.001 & 0.001 \\ 3.001 & 0.001 & 2.001 \end{pmatrix}$$

and

$$\boldsymbol{\theta} = (0.0129, 0.0162, 0.0229, 0.0356, 0.0343, 0.0114, 0.0171, 0.0113, 0.0227, 0.0227, 0.0227, 0.0356, 0.0388, 0.0514, 0.7995, 0.0210, 0.0405, 0.0514, 0.0097, 0.0227, 0.0243, 0.0178, 0.0113, 0.0405, 0.0857, 0.0388, 0.0307, 0.0743, 0.0210, 0.0457, 0.1600, 0.0400, 0.0743, 0.0194, 0.0743, 0.0210, 0.1999, 0.0243, 0.0243, 0.0210, 0.0324, 0.0259, 0.0291, 0.0000, 0.0129, 0.0343, 0.0000, 0.0113, 0.0097, 0.0514, 0.0457, 0.0227, 0.0049, 0.0194, 0.0049, 0.0194, 0.0243, 0.0800, 0.0343, 0.0129, 0.0049, 0.0081, 0.0114, 0.0340, 0.0372, 0.0259, 0.0081, 0.0146, 0.0097, 0.0113, 0.0097).$$

(d) **Practice.** For groups created according to practice, we test an ERMM with

$$\mathbf{n} = (41, 30) \text{ and } \mathbf{Q} = \begin{pmatrix} 0.2060 & 0.1268 \\ 0.1268 & 0.1701 \end{pmatrix}.$$

For a corresponding DCSBM we use

$$\mathbf{n} = (41, 30), \quad \mathbf{Q} = \begin{pmatrix} 338.001 & 156.001 \\ 156.001 & 148.001 \end{pmatrix}$$

and

$$\boldsymbol{\theta} = (0.0162, 0.0329, 0.0081, 0.0724, 0.0121, 0.0040, 0.0099, 0.0142, 0.0461, 0.0461, 0.0283, 0.0724, 0.0486, 0.0296, 0.0132, 0.0428, 0.0822, 0.0182, 0.0197, 0.0283, 0.0304, 0.0223, 0.0142, 0.0506, 0.0493, 0.0486, 0.0385, 0.0428, 0.0428, 0.0162, 0.0567, 0.0142, 0.0263, 0.0395, 0.0428, 0.0263, 0.0033, 0.0304, 0.0304, 0.0263, 0.0405, 0.0526, 0.0364, 0.0000, 0.0263, 0.0197, 0.0000, 0.0230, 0.0121, 0.0296, 0.0162, 0.0283, 0.0099, 0.0243, 0.0061, 0.0243, 0.0304, 0.0283, 0.0121, 0.0263, 0.0099, 0.0164, 0.0066, 0.0691, 0.0466, 0.0324, 0.0101, 0.0182, 0.0121, 0.0230, 0.0121).$$

(e) **Law school.** For groups created according to which law school the person attended, we test an ERMM with

$$\mathbf{n} = (15, 28, 28) \text{ and } \mathbf{Q} = \begin{pmatrix} 0.2571 & 0.1476 & 0.1190 \\ 0.1476 & 0.2089 & 0.1696 \\ 0.1190 & 0.1696 & 0.1269 \end{pmatrix}.$$

For a corresponding DCSBM we use

$$\mathbf{n} = (15, 28, 28), \quad \mathbf{Q} = \begin{pmatrix} 54.001 & 62.001 & 50.001 \\ 62.001 & 158.001 & 133.001 \\ 50.001 & 133.001 & 96.001 \end{pmatrix}$$

and

$$\boldsymbol{\theta} = (0.0482, 0.0602, 0.0241, 0.0789, 0.0170, 0.0120, 0.0108, 0.0251, 0.0843, 0.0502, 0.0843, 0.0623, 0.0680, 0.0542, 0.0143, 0.0783, 0.1506, 0.0255, 0.0361, 0.0843, 0.0425, 0.0394, 0.0198, 0.0708, 0.0425, 0.0860, 0.1145, 0.0368, 0.0466, 0.0287, 0.0793, 0.0251, 0.0466, 0.0340, 0.0466, 0.0466, 0.0036, 0.0425, 0.0904, 0.0783, 0.0567, 0.0453, 0.0510, 0.0000, 0.0287, 0.0170, 0.0000, 0.0251, 0.0170, 0.0255, 0.0287, 0.0502, 0.0108, 0.0430, 0.0108, 0.0340, 0.0425, 0.0502, 0.0170, 0.0227, 0.0108, 0.0142, 0.0057, 0.0595, 0.0824, 0.0573, 0.0142, 0.0323, 0.0215, 0.0198, 0.0170).$$

Table 5: Goodness of fit results for testing the fit of IRG models on Lazega’s lawyers networks (using WL with $h = 2$)

| Network | Group labels | ERMM | | DCSBM | |
|------------|--------------|---------------------------|---------|---------------------------|---------|
| | | IRG-gKSS ² | P-value | IRG-gKSS ² | P-value |
| Work | Single group | 0.5652 (0.4003,0.5951) | 0.1692 | - | - |
| Advice | Single group | 3.424 (2.947,3.639) | 0.5174 | - | - |
| Friendship | Single group | 0.7064 (0.4681,0.6997) | 0.0597 | 0.5624 (0.3678,0.5343) | 0.0299 |
| | Status | 0.5973 (0.3977,0.6224) | 0.0995 | 0.4526 (0.2772,0.4030) | 0.0299 |
| | Gender | 0.6833 (0.4388,0.6534) | 0.0299 | 0.5423 (0.3502,0.5115) | 0.0398 |
| | Office | 0.6230 (0.4506,0.6408) | 0.0995 | 0.4763 (0.2922,0.4213) | 0.00995 |
| | Practice | 0.6833 (0.4311,0.6577) | 0.0299 | 0.5407 (0.3513,0.5162) | 0.0299 |
| | Law school | 0.6767 (0.4447,0.6678) | 0.0498 | 0.5382 (0.3366,0.5171) | 0.00995 |
| | | | | | |

Table 6: Goodness of fit results for testing the fit of IRG models on Lazega’s lawyers’ friendship network (using WL with $h = 3$)

| Group labels | ERMM | | DCSBM | |
|--------------|--------------------------|---------|------------------------|---------|
| | IRG-gKSS ² | P-value | IRG-gKSS ² | P-value |
| Gender | 4.504 (4.852,5.977) | 0.00995 | 3.201 (2.762,3.457) | 0.6467 |
| Practice | 4.507 (4.815,5.927) | 0.00995 | 3.200 (2.718,3.552) | 0.6368 |
| Law school | 4.44339 (4.741,5.895) | 0.01990 | 3.169 (2.716,3.602) | 0.8557 |

As an aside, from Table 3 we see that for an IRG model in which communities are created using the office where the lawyers work, the discrepancy between the ER and the corresponding ERMM is higher than the discrepancy between ERMM and a corresponding DCSBM.

Table 7: GLR tests between IRG models for Lazega’s lawyers’ friendship network, with the 5% critical value from the approximating chi-square distribution in parentheses. The degrees of freedom are $k = 2$ for Status, Gender, and Practice, and $k = 5$ for Office and Law school, for the tests of ER against ERMM. For the tests of ERMM against DCSBM, the degrees of freedom are $k = 69$ for Status, Gender, and Practice, and $k = 68$ for Office and Law school.

| Group labels | GLR test statistic and $\chi_k^2(\alpha)$ | |
|--------------|---|--------------------|
| | ER against ERMM | ERMM against DCSBM |
| Status | 333.2 (5.991) | 685.4 (89.39) |
| Gender | 45.94 (5.991) | 710.7 (89.39) |
| Office | 474.9 (11.07) | 550.2 (88.25) |
| Practice | 46.21 (5.991) | 704.5 (89.39) |
| Law school | 45.30 (11.07) | 696.60 (88.25) |

In a related experiment, reported in Table 7, we used a likelihood ratio test for the Status network to test the ERMM model against the ER model; the test rejected the ER model in favour of the ERMM model. Then we tested the DCSBM model against the ERMM model; the test rejected the ERMM model in favour of the DCSBM model. This experiment makes it clear that, in contrast to the IRG-gKSS test, the likelihood ratio test is not a goodness-of-fit test against the general alternative; rather, the results depend on the specified alternative model.

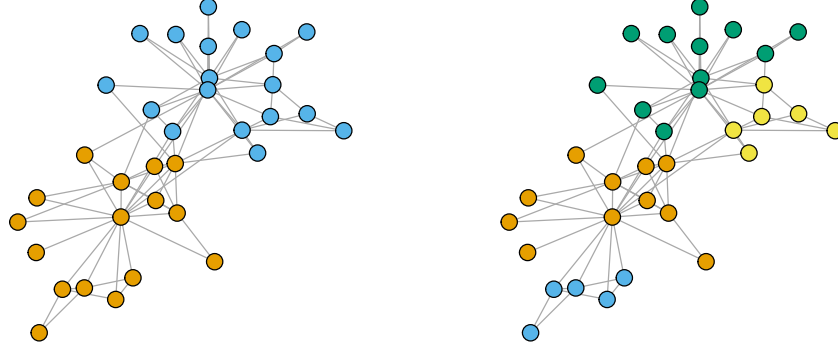


Figure 23: Zachary's Karate club network (left) with the observed split into two groups and (right) the network with 4 groups.

F.3 The Karate club network

Here we give further details about the Karate club network example from Section 4.2.2 of the main text, with $n = 34$ vertices. For ER and ERMM models, we use the maximum likelihood estimates from the observed network as parameters in the null model, namely $p = 0.139$ for the ER model; for the ERMM model, we take two groups reflecting the split, with sizes $\mathbf{n}_1 = (16, 18)$, and parameter estimates

$$\mathbf{Q}_1 = \begin{pmatrix} 0.2750 & 0.0347 \\ 0.0347 & 0.2288 \end{pmatrix}.$$

We also test an ERMM model with four communities as suggested in Karwa et al. [2024]. Figure 23 shows the groups for both the observed split and the output from the Louvain algorithm with the highest modularity.

The maximum likelihood estimates of the parameters of an ERMM model with four groups are $\mathbf{n}_2 = (11, 5, 12, 6)$ and

$$\mathbf{Q}_2 = \begin{pmatrix} 0.4182 & 0.0727 & 0.0530 & 0.0455 \\ 0.0727 & 0.6000 & 0.0000 & 0.0000 \\ 0.0530 & 0.0000 & 0.3182 & 0.0972 \\ 0.0455 & 0.0000 & 0.0972 & 0.4667 \end{pmatrix},$$

which we use as parameters in the null model for testing the fit of an ERMM with four groups.

For the DCSBM, we estimate the parameters 'DCSBM.estimate' function from the `randnet` package in R. The estimates are $\mathbf{n} = (16, 18)$, $\mathbf{Q} = \begin{pmatrix} 66.001 & 10.001 \\ 10.001 & 70.001 \end{pmatrix}$ and

$$\boldsymbol{\theta} = (0.2105, 0.1184, 0.1316, 0.0789, 0.0395, 0.0526, 0.0526, 0.0526, 0.0625, 0.0250, 0.0395, 0.0132, 0.0263, 0.0658, 0.0250, 0.0250, 0.0263, 0.0263, 0.0250, 0.0395, 0.0250, 0.0263, 0.0250, 0.0625, 0.0375, 0.0375, 0.0250, 0.0500, 0.0375, 0.0500, 0.0500, 0.0750, 0.1500, 0.2125).$$

We use $p_{u,v} = 1 - e^{-Q_{gu,gv}\theta_u\theta_v}$ for all u and v in the network as null parameters to test the fit of a DCSBM.

F.4 Padgett's Florentine marriage network

As another real-world example, we consider the subgraph of the Florentine marriage data from Padgett [1987] constructed in Breiger and Pattison [1986]. It consists of 20 marriage ties (edges) between 16 families (vertices) in Florence, Italy. The data set contains two more variables for the families in the network: net wealth in 1427, and the number of seats on the city council from 1288–1344.

Table 8: Testing the fit of some IRG models on Zachary’s Karate club network (using WL with $h = 2$)

| | Model | | | |
|-----------------------|----------------------------|------------------------------------|------------------------------------|---|
| | $ER(n, p)$ | $ERMM(\mathbf{n}_1, \mathbf{Q}_1)$ | $ERMM(\mathbf{n}_2, \mathbf{Q}_2)$ | $DCSBM(\mathbf{n}, \mathbf{Q}, \theta)$ |
| IRG-gKSS ² | 0.4254 (0.1296, 0.3482) | 0.3077 (0.1097, 0.2382) | 0.2453 (0.0848, 0.1887) | 0.1921 (0.0601, 0.1292) |
| P-value | 0.02985 | 0.00995 | 0.00995 | 0.00995 |

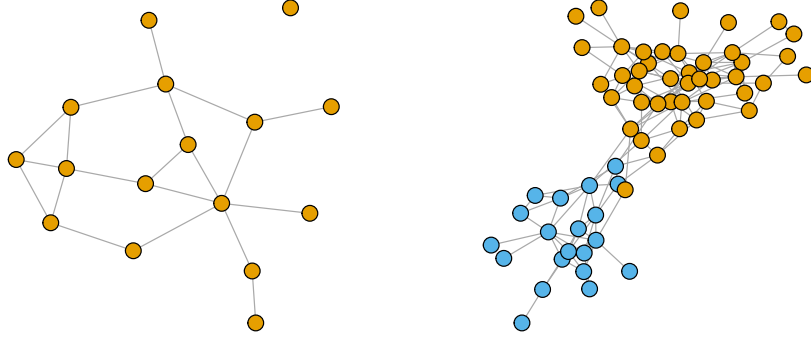


Figure 24: Left: Florentine marriage network; right: Dolphin network.

We test the fit of the Erdős-Rényi (ER) random graph model with $n = 16$ and $p_0 = 20/120 = 1/6$ on this network. The results in Table 9 show that the IRG-gKSS test does not reject the fit of an $ER(16, 1/6)$ model to the Florentine marriage network. This finding agrees with the finding in Xu and Reinert [2021]. As the GLR test requires specifying an alternative, we did not employ it here.

F.5 Lusseau’s dolphin network

As a final real-world example, we consider the social network of bottlenose dolphins in Doubtful Sound, New Zealand, from Lusseau et al. [2003], constructed from observations of a community of 62 bottlenose dolphins over seven years from 1994 to 2001. The vertices in the network represent the dolphins, and the undirected edges between the vertices represent associations between a pair of dolphins occurring more often than expected by chance.

This network is one of the benchmark networks in social network analysis. Lusseau [2003] argues that the connectivity of individuals follows a complex distribution that has a scale-free power-law distribution for large degrees k . Jin et al. [2013] and Caimo and Friel [2011] found that the dolphin network is inhomogeneous; a few vertices have higher degrees while others have only one or two edges. They analysed this network using an ERGM with the degree and shared partnership statistics. Ouyang et al. [2023] fits a mixed membership model to the dolphin network. None of these papers assessed the fit of the suggested model using a statistical test procedure.

Here we test the fit of IRG models to the dolphin network. The results of IRG-gKSS, given in Table 9, show that we do not reject the fit of an $ER(62, 0.0841)$ for the dolphin network. An ER network model would be a much simpler explanation for the data than those previously suggested. Investigating this discrepancy further will be part of future work.

Table 9 shows that for the Florentine marriage network and for the dolphin network, the number of iterations (or height) of the WL kernel does not affect the conclusion of the test. It does, however, affect the P -value. Moreover, it illustrates that the IRG-gKSS value increases with h as each iteration increases the WL values.

Table 9: Testing the fit to an ER model for the Florentine marriage network and the dolphin network (using a WL kernel with $h = 2$ and with $h = 3$)

| Network | Model | $h = 2$ | | $h = 3$ | |
|---------------------|----------------|-------------------------------|---------|----------------------------|---------|
| | | IRG-gKSS ² | P-value | IRG-gKSS ² | P-value |
| Florentine Marriage | ER(16, 1/6) | 0.3119 (0.1119, 0.6506) | 0.8557 | 1.042 (0.3613, 1.981) | 0.9651 |
| Dolphin | ER(62, 0.0841) | 0.06981 (0.04740, 0.09535) | 0.7860 | 0.5258 (0.4641, 0.9899) | 0.1791 |